Heavy flavor spectroscopy and exotic hadrons at LHC

Roberta Cardinale
on behalf of the LHCb collaboration
with results from ATLAS and CMS

DIS 2019
Torino - 8 -10 April 2019

Heavy flavour spectroscopy at LHC

- Thanks to the large centre-of-mass energy, LHC provides a large amount of $b\bar{b}$ and $c\bar{c}$ pairs
  - $\sim 10^{11} b\bar{b}$/yr in forward region
  - 20 times more for $c\bar{c}$
- Important as tests and inputs to QCD models
  - Various theoretical models make predictions on the heavy hadron production and properties
  - New states/decays provide inputs to theory
  - Many observed states still lack of interpretation: exotic states which are not fitting the standard picture
- But also to be able to fully understand processes which are the Standard Model background in the search for new physics

LHCb, ATLAS and CMS experiments

- LHCb, ATLAS and CMS are complementary in heavy flavour spectroscopy studies
  - ATLAS and CMS cover high p_{T} and low rapidity range
  - LHCb covers low p_{T} and higher rapidity region
    - In addition LHCb has an excellent vertexing and particle identification capabilities: dedicated to heavy flavour physics

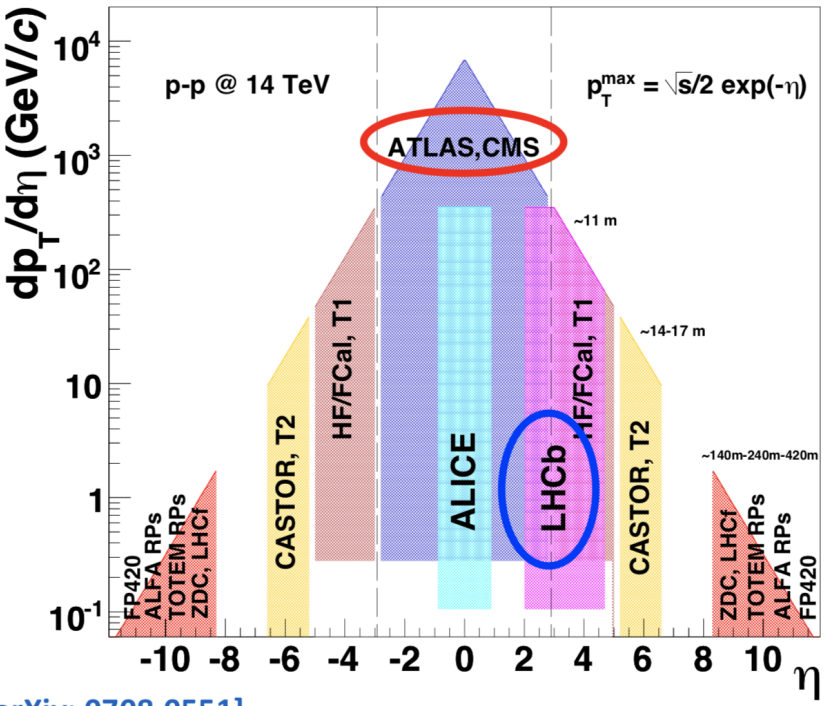

[arXiv: 0708.0551]

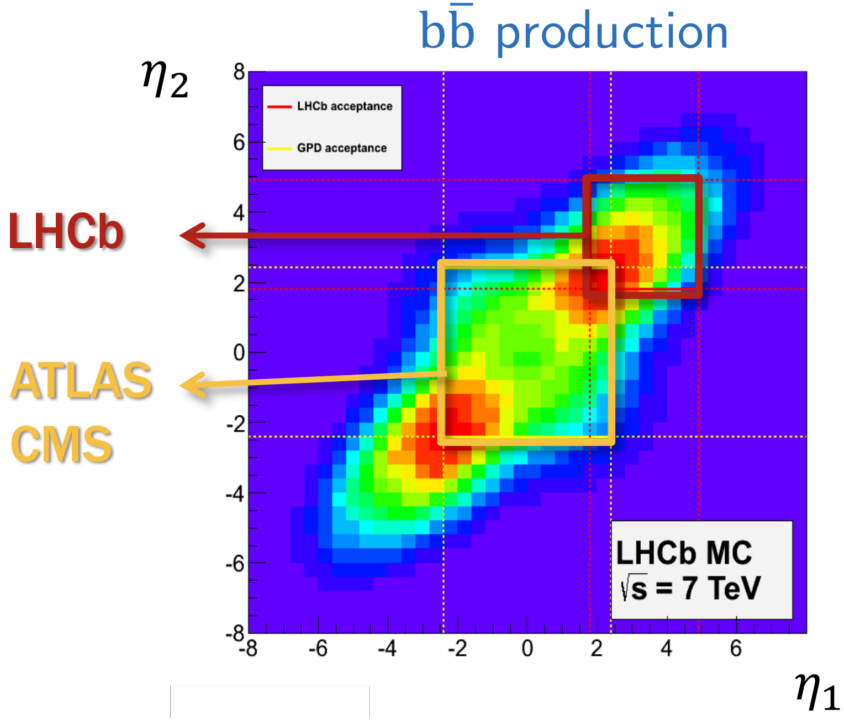

Exotic spectroscopy

- The observation of states with properties inconsistent with pure $c\bar{c}$ and $b\bar{b}$ states raised the interest of the so-called exotic (non-standard) quarkonium states from both the theoretical and experimental point of view starting from the discovery of the $X(3872)$ state
- Since then, a plethora of unexpected neutral (X, Y) and charged (Z^+, P_c^+) states have been discovered
- The nature and the internal structure of these states are still unclear (molecular/tightly bound): many efforts needed to uncover their nature

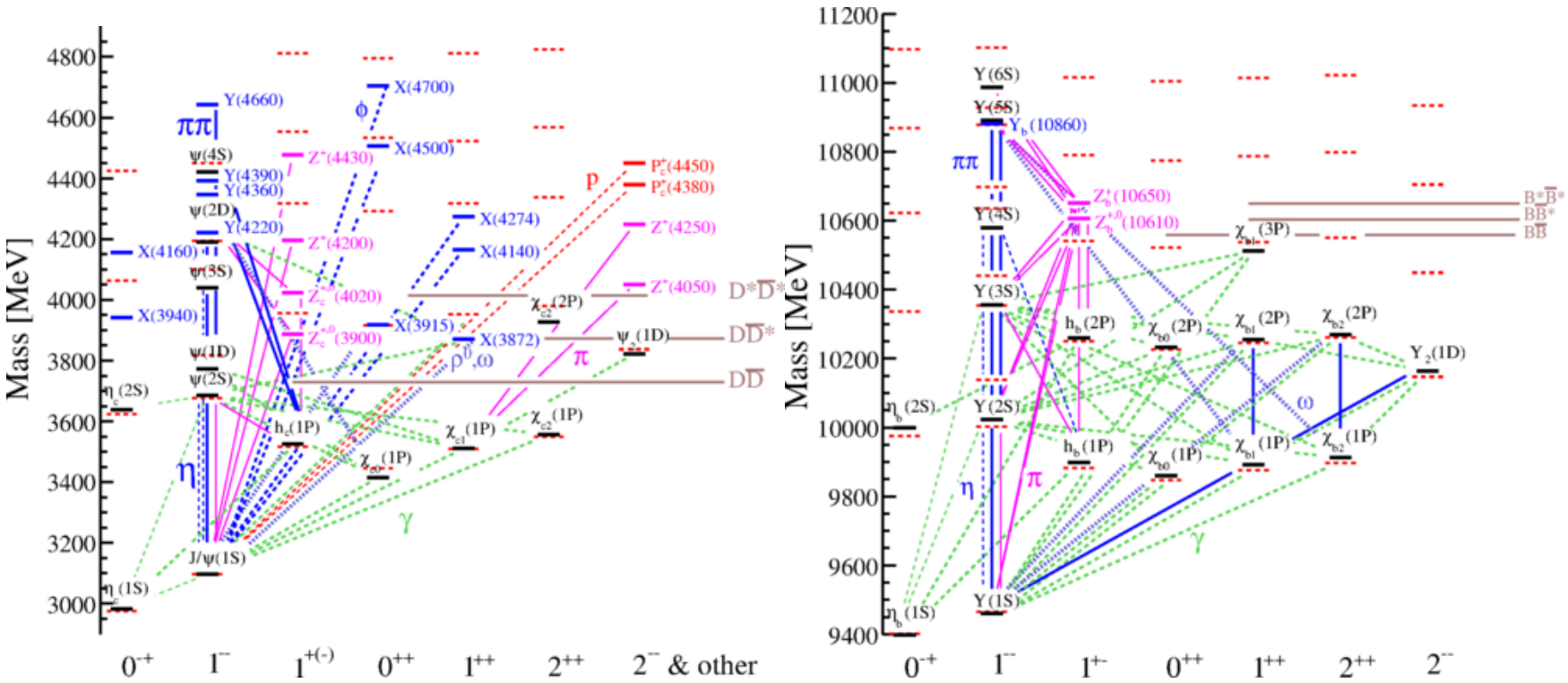

[Rev.Mod.Phys 90 (2018) 015003]

Evidence for an $\eta_c(1S)\pi^-$ resonance in $B^0 \to \eta_c(1S)K^+\pi^-$ decays

EPJC 78 (2018) 1019

$\eta_c\pi^-$ resonance in $B^0 \to \eta_c K^+\pi^-$: motivations

- Predictions of $\eta_c\pi^-$ states depending on the model used to describe the $Z_c(3900)^-$ discovered by BESIII [PRL 110 (2013) 252001]
  - hadrocharmonium state: charged charmonium-like state of mass $\sim 3800\,\mathrm{MeV}$ [PRD87 (2013) 091501]
  - quarkonium hybrids: prediction of states with quantum numbers allowing the decay into the $\eta_c\pi^-$ system
- Using the diquark model: a $J^P = 0^+$ exotic candidate below the open-charm threshold decaying to $\eta_c\pi^-$ [PRD71 (2005) 014028]

Search for possible exotic states in the $\eta_c\pi^-$ invariant mass using $B^0 \to \eta_c K^+\pi^-$ decays

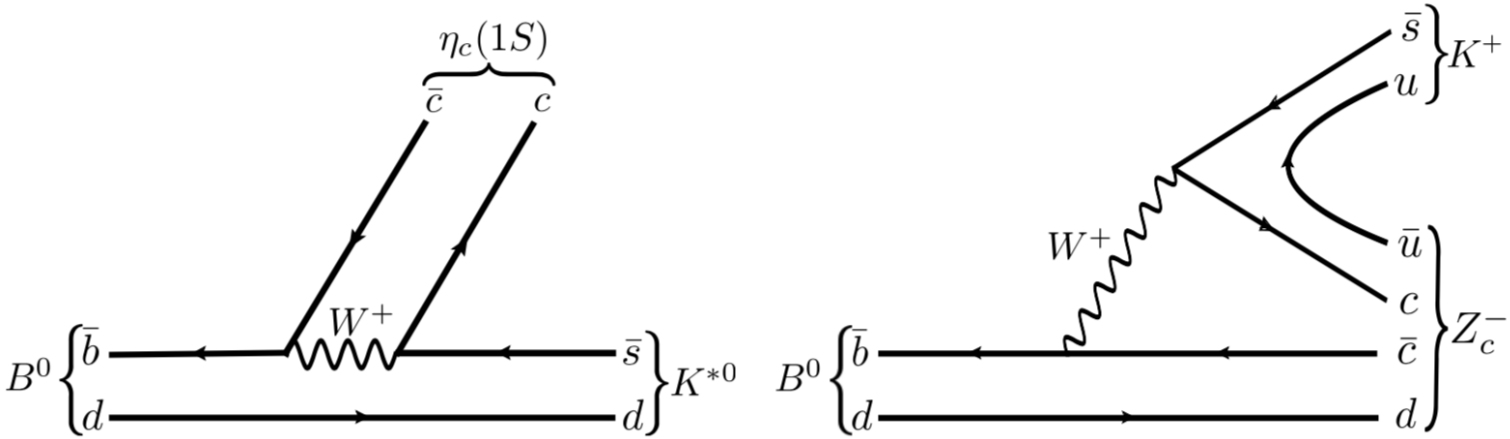

$B^0 \to \eta_c(1S)K^+\pi^-$: analysis strategy [EPJC 78 (2018) 1019]

- Using $L \sim 4.7\,\text{fb}^{-1}$, Run1+Run2 data (2011-2016)
- η_c reconstructed in $p\bar{p}$ final state
- isolate $B^0 \to \eta_c K^+\pi^-$ signal candidates from non-resonant $B^0 \to p\bar{p}K^+\pi^-$ and combinatorial background candidates
- Perform a Dalitz plot (DP) analysis to search for exotic hadrons: the $B^0 \to \eta_c(1S)K^+\pi^-$ decay involves only pseudo-scalar particles (fully described by only two independent kinematic quanties)
- Isobar model used to write the decay amplitude: $K^+\pi^-$ S-wave at low mass parametrised using the LASS PDF, Breit Wigner PDFs for the other $K^+\pi^-$ resonances

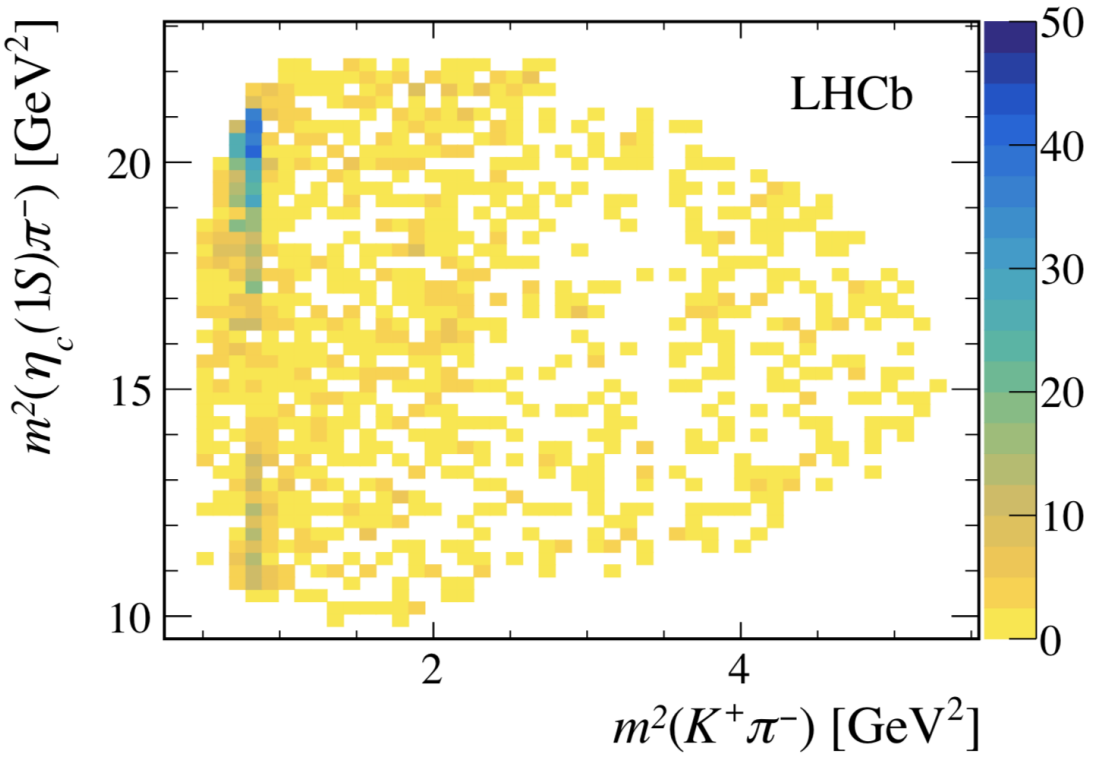

$B^0 \to \eta_c(1S)K^+\pi^-$: signal [EPJC 78 (2018) 1019]

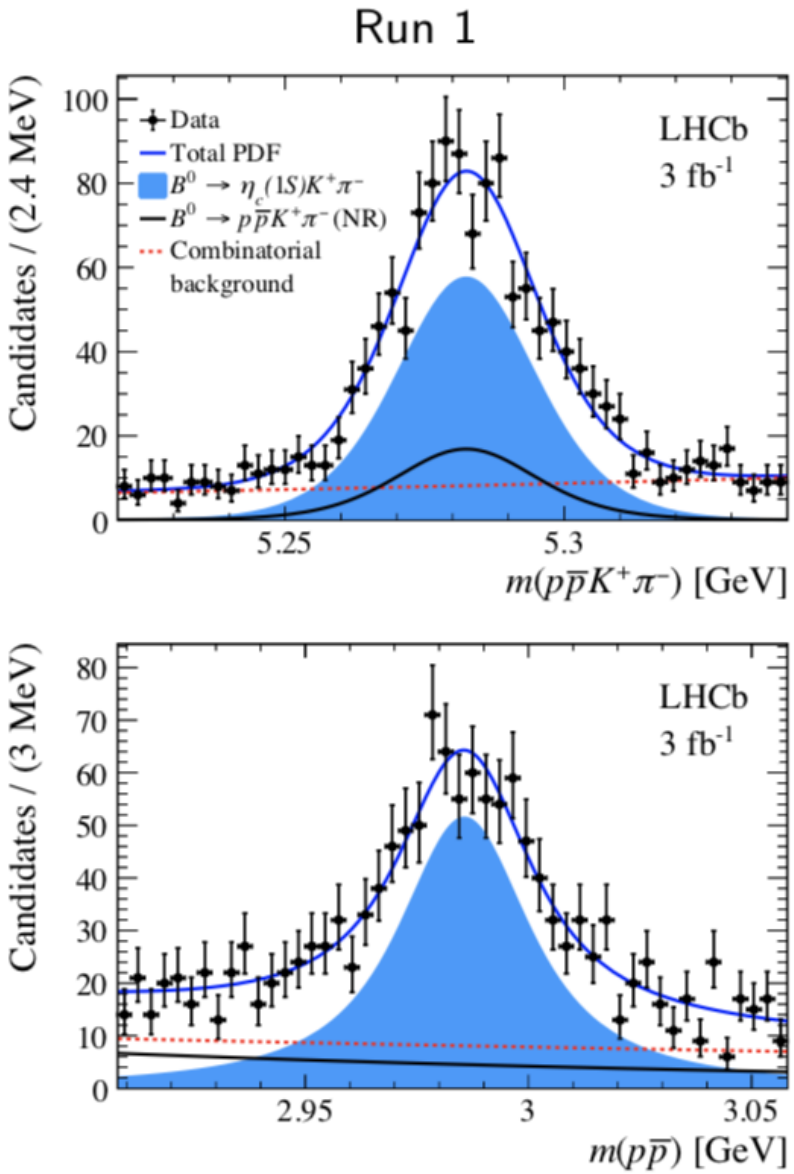

- 2D fit to $m(p\bar{p}K^+\pi^-)$ and $m(p\bar{p})$ distributions
- to subtract non-resonant $B^0 \to p\bar{p}K^+\pi^-$ and combinatorial background candidates
- fitting separetely Run1 and Run2 data

Component	Run 1	Run 2
$B^0 \to \eta_c K^+\pi^-$	805 ± 48	1065 ± 56
$B^0 \to p\bar{p}K^+\pi^-$ (NR)	234 ± 48	273 ± 56
Combinatorial background	409 ± 36	498 ± 41

Dalitz plot analysis [EPJC 78 (2018) 1019]

- Background: use sPlot technique to get the nonresonant and combinatorial background distributions (included in the amplitude fit)
- Efficiency:
  - variation caused by the detector acceptance and selection procedure
  - parametrisation using re-weighted simulated samples
- Baseline model includes 6 K^{*0} resonances + $K^+\pi^-$ NR (mass and width of each K^* resonance are fixed)

Resonance	Mass [MeV]	Width [MeV]	J^P	Model
$K^*(892)^0$	895.55 ± 0.20	47.3 ± 0.5	1^-	RBW
$K^*(1410)^0$	1414 ± 15	232 ± 21	1^-	RBW
$K_0^*(1430)^0$	1425 ± 50	270 ± 80	0^+	LASS
$K_2^*(1430)^0$	1432.4 ± 1.3	109 ± 5	2^+	RBW
$K^*(1680)^0$	1717 ± 27	322 ± 110	1^-	RBW
$K_0^*(1950)^0$	1945 ± 22	201 ± 90	0^+	RBW

Model with only $K^+\pi^-$ contributions [EPJC 78 (2018) 1019]

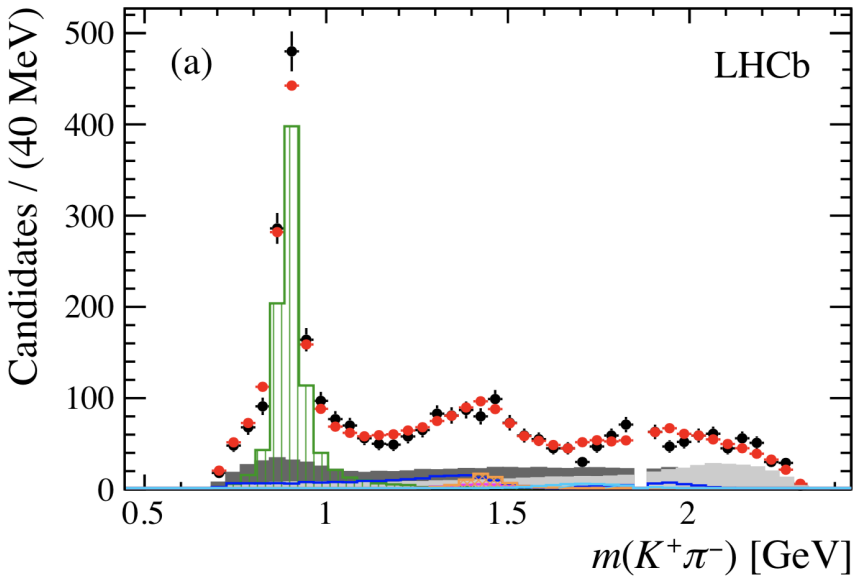

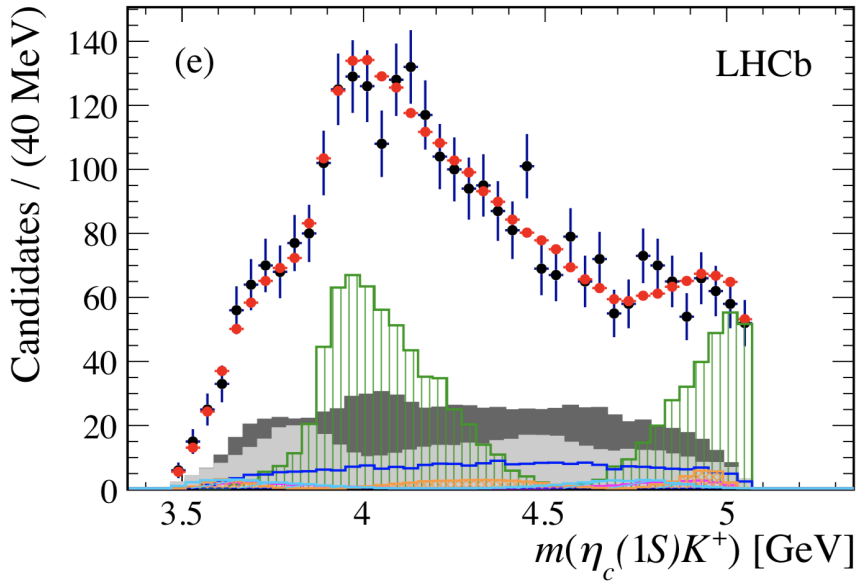

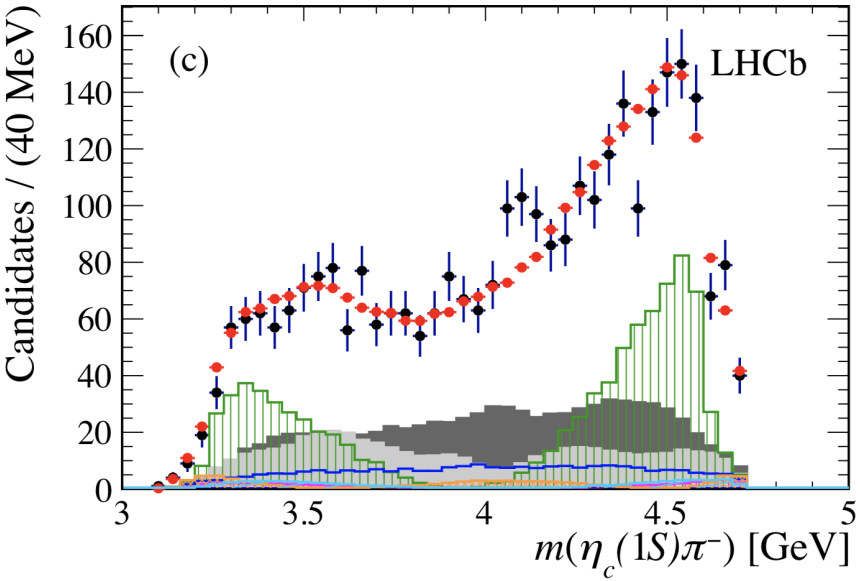

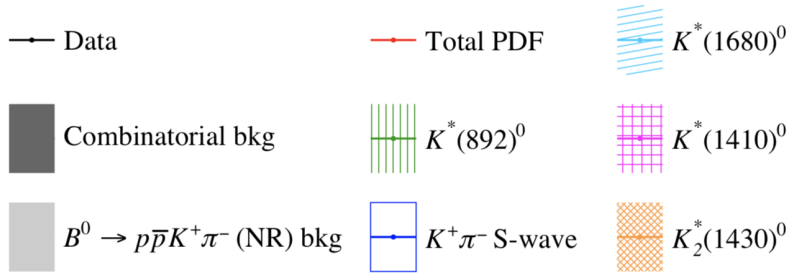

Discrepancy around $4100\,\mathrm{MeV}$ in the $m(\eta_c(1S)\pi^-)$ spectrum

Model with $K^+\pi^- + \eta_c(1S)\pi^-$ [EPJC 78 (2018) 1019]

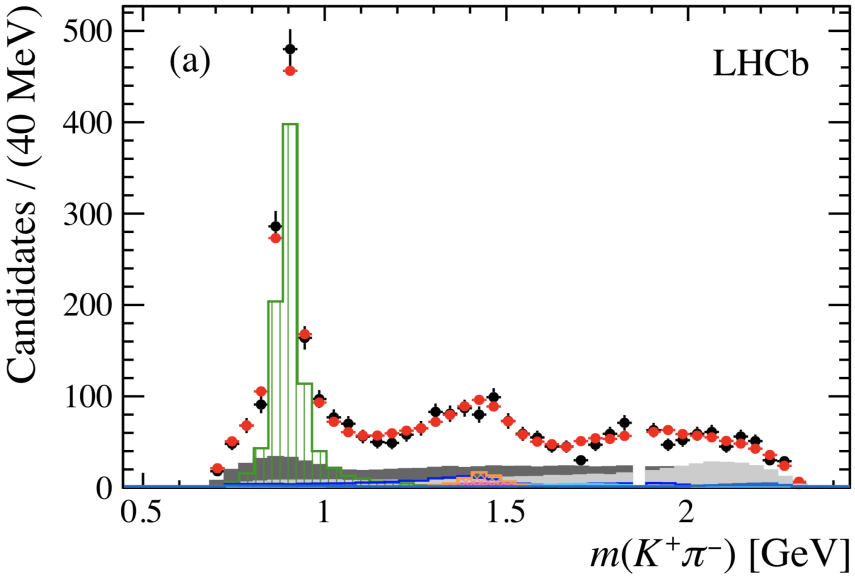

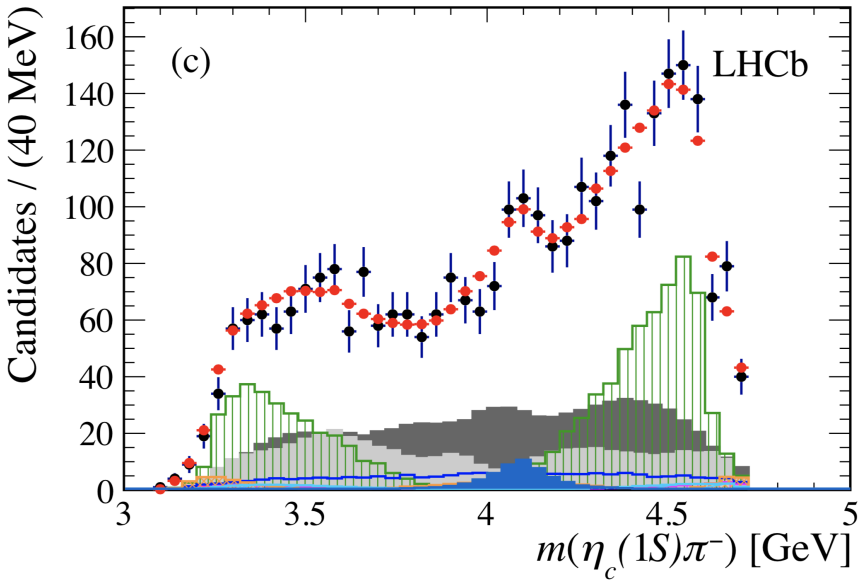

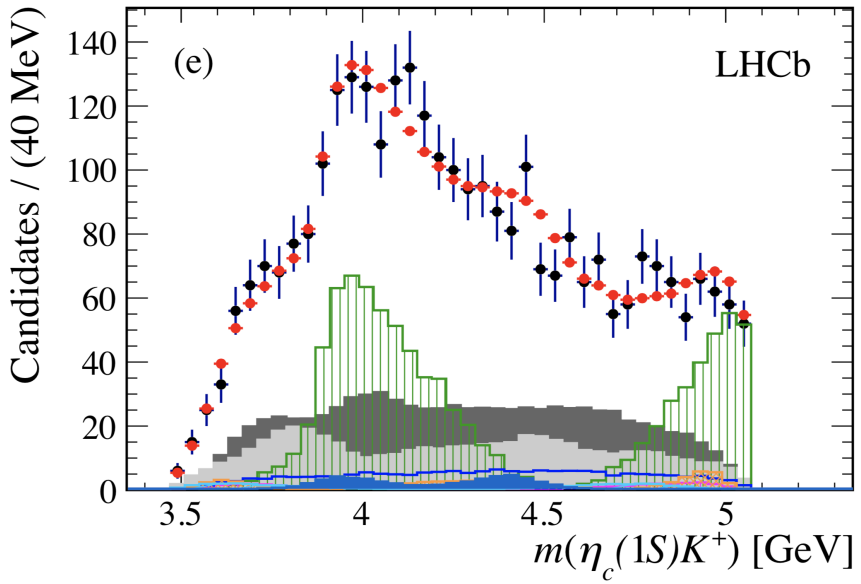

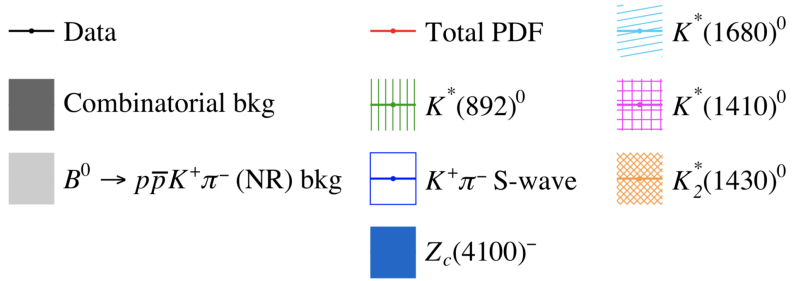

Evidence for an exotic $Z_c(4100)^-$ [EPJC 78 (2018) 1019]

- Adding a Z_c^- resonance improves the fit of $\Delta(2ln\mathcal{L}) = 22.8$, 41.4 and 7.0 for $J^P = 0^+$, 1^- and 2^+.
- Resonance parameters:

$$m_{Z_c^-} = 4096 \pm 20^{+18}_{-22}\,\text{MeV}$$
$$\Gamma_{Z_c^-} = 152 \pm 58^{+60}_{-35}\,\text{MeV}$$

- Fit fraction of the Z_c^-: $3.3 \pm 1.1^{+1.2}_{-1.1}\%$
- $\mathcal{B}(B^0 \to Z_c(4100)^- K^+) = 1.89 \pm 0.64 \pm 0.04^{+0.69}_{-0.63} \pm 0.22$
  (statistical, branching fraction systematic, fit fraction systematic, external branching fractions uncertainties)
- Significance is 3.2σ after considering systematic uncertainties
- Discrimination between $J^P = 0^+$ and $J^P = 1^-$ is not significant

Exotic contributions to $B^0 \to J/\psi K^+\pi^-$

arXiv:1901.05745, Submitted to PRL

Exotics in $B^0 \to J/\psi K^+\pi^-$ at LHCb [arXiv:1901.05745]

- Belle reported an exotic state $Z_c(4200)^- \to J/\psi\pi^-$ [PRD 90(2014) 112009]
- BaBar did not confirm this state [PRD 79 (2009) 112001]
- Angular analysis at LHCb using $3\,\mathrm{fb}^{-1}$ Run1 data

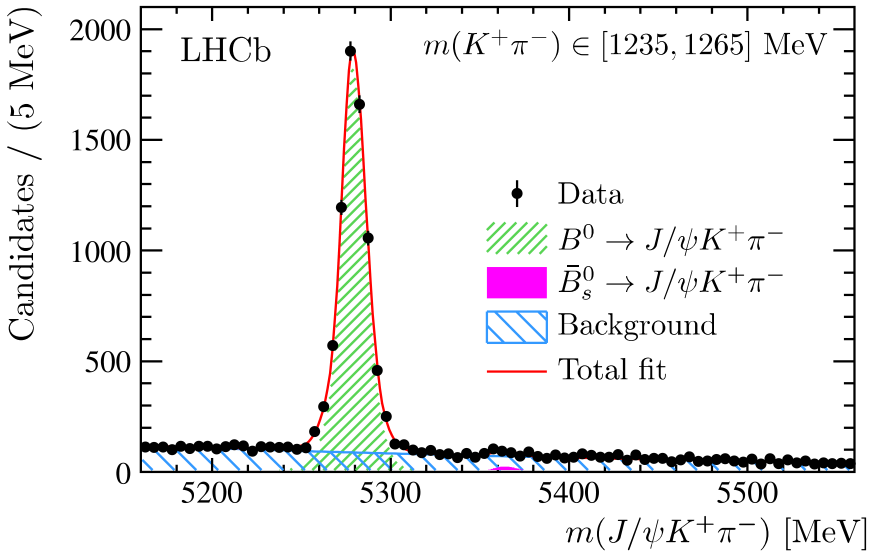

- $N(B^0 \to J/\psi K^+\pi^-) = 554500 \pm 800$ in $m(K^+\pi^-) \in [745, 1545]\,\mathrm{MeV}$ ($\times 20$ and $\times 40$ larger than Belle and BaBar dataset)
- Model independent 4D analysis with minimal assumptions on the K^*_j spectrum to avoid large systematics due to the poor understanding of K^*_j resonances
  - Data divided in $m(K^+\pi^-)$ bins
  - Check in each bin if the 3D angular distribution can be described only by conventional K^*_j states without including an exotic component
  - Requiring only knowledge of the highest spin $J_{\max}$ among all the contributing K^*_j states, for a given $m(K^+\pi^-)$ bin

Exotics in $B^0 \to J/\psi K^+\pi^-$ at LHCb [arXiv:1901.05745]

- K_j^*-only hypothesis rejected with a significance of 10σ

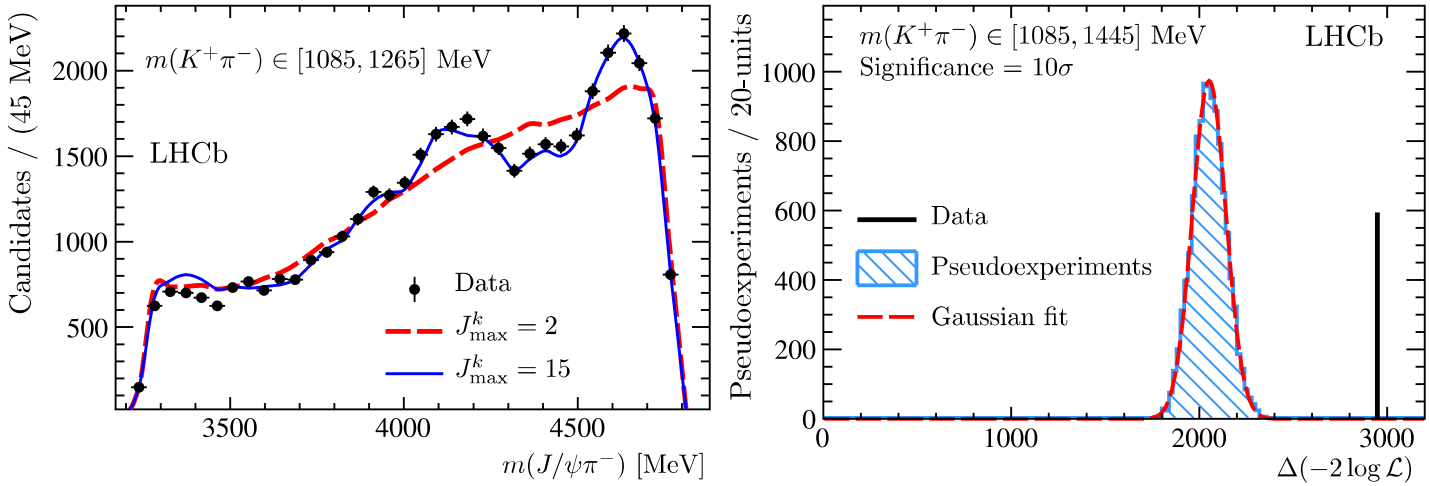

- $(m(J/\psi\pi^-), m(K^+\pi^-))$ 2D plot: structures visible around $m(J/\psi\pi^-) \sim 4200\,\text{MeV}$ and $m(J/\psi\pi^-) \sim 4600\,\text{MeV}$

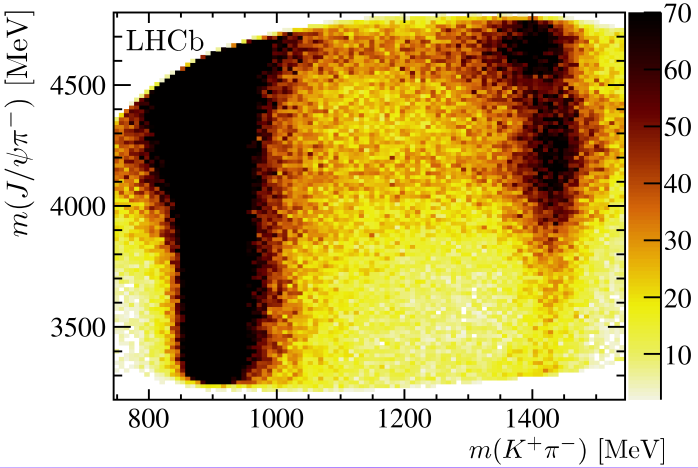

Pentaquarks

LHCb-PAPER-2019-014 (in preparation)

Pentaquarks in $\Lambda_b^0 \to J/\psi p K^-$ using Run1 $3\,\mathrm{fb}^{-1}$ data [PRL 115 (2015) 072001, PRL 117 (2016) 082002]

- Clean signal of 26000 candidates with 5.4% background
- Dalitz plot has unusual features: unexpected narrow peak in the $m_{J/\psi p}$ at $19.5\,\mathrm{GeV}^2$
- Resonances in $m_{J/\psi p}$ have a minimum quark content of $c\bar{c}uud$
- Six-dimensional amplitude fit allowing for two interfering channels: $\Lambda_b^0 \to J/\psi \Lambda^*$ and $\Lambda_b^0 \to P_c^+ K^-$ + model independent analysis
- Two exotic states with opposite parities

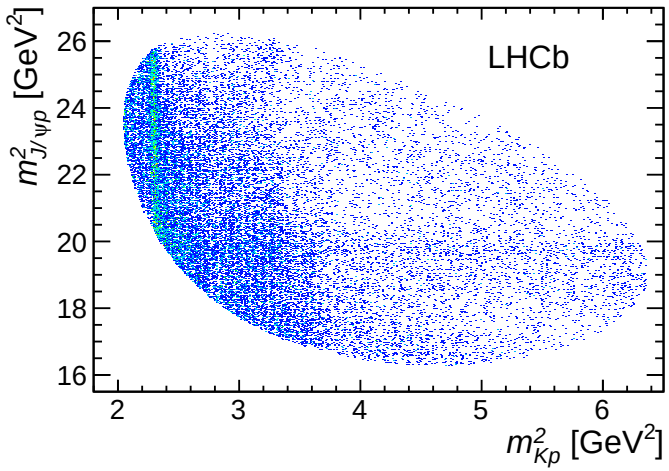

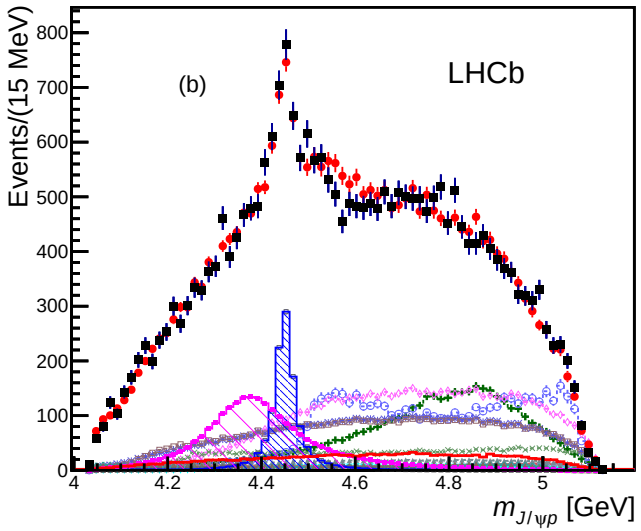

	$P_c(4380)^+$	$P_c(4450)^+$
J^P	$\frac{3}{2}^-$	$\frac{5}{2}^+$
Mass [MeV/c^2]	$4380 \pm 8 \pm 29$	$4449.8 \pm 1.7 \pm 2.5$
Width [MeV/c^2]	$205 \pm 18 \pm 86$	$39 \pm 5 \pm 19$
Fit fraction [%]	$8.4 \pm 0.7 \pm 4.2$	$4.1 \pm 0.5 \pm 1.1$
Significance	9σ	12σ

Pentaquark update [LHCb-PAPER-2019-014 (in preparation)]

- 246k $\Lambda_b \to J/\psi p K^-$: 9x wrt Run1 candidates
- 6D amplitude fit consistent between Run1 and Run2 data
- A fine binning shows more $J/\psi p$ structures which were not significant in the Run1 analysis
  - Narrow peak at $4312\,\mathrm{MeV}$ with a width comparable to the mass resolution ($\sim 2 \div 3\,\mathrm{MeV}$)
  - The structure at $4450\,\mathrm{MeV}$: resolved into two narrow peaks at $4440\,\mathrm{MeV}$ and $4457\,\mathrm{MeV}$

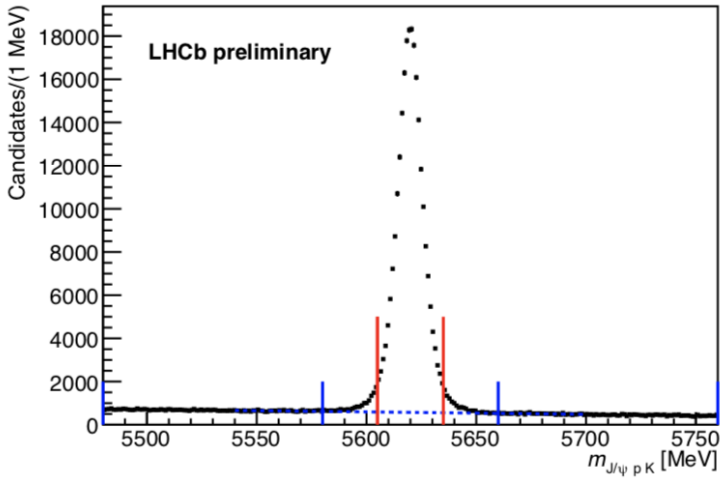

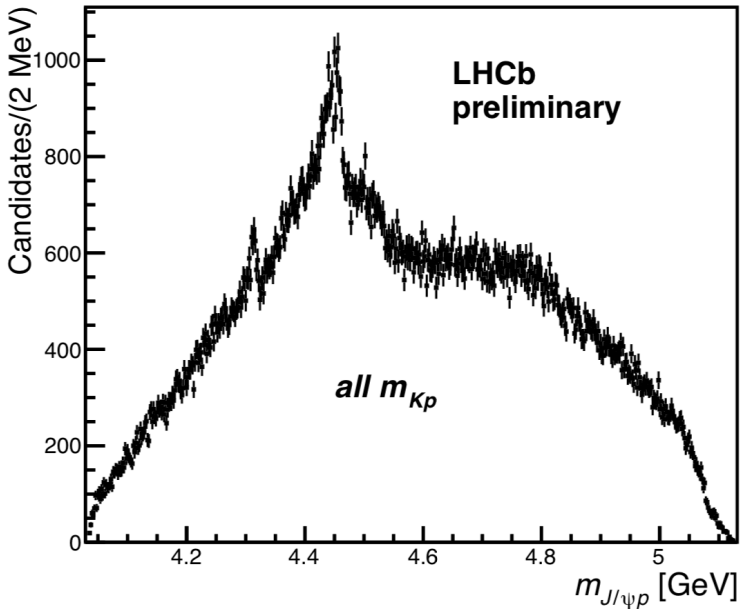

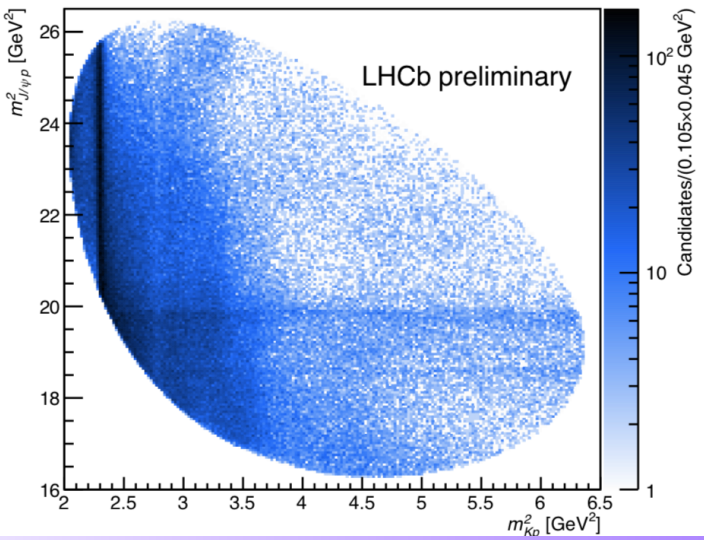

Pentaquark update [LHCb-PAPER-2019-014 (in preparation)]

- Suppression of Λ^* resonances requiring $m_{Kp} > 1.9\,\mathrm{GeV}$

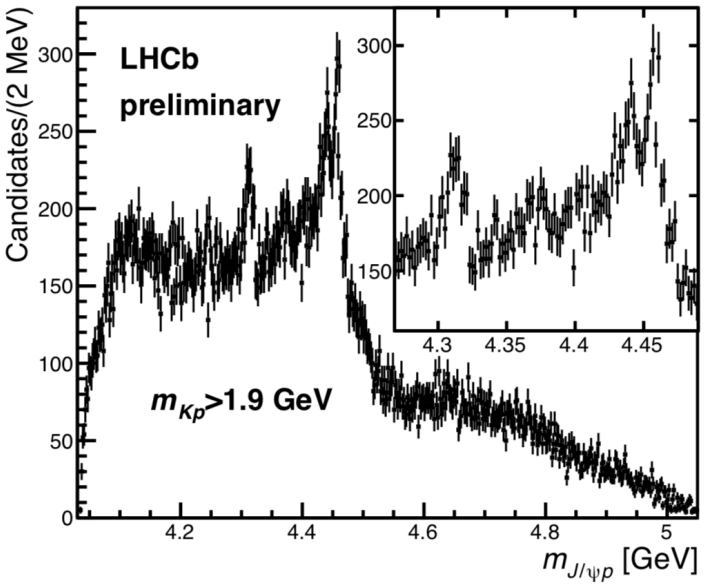

- Amplitude analysis is challenging (size of the data sample, amplitude model formulation, mass resolution)
- For narrow peaks, perform one-dimensional fits to $m_{J/\psi p}$

Three BW + high-order polynomial low-order polynomial

Different Λ^* reflection compositions

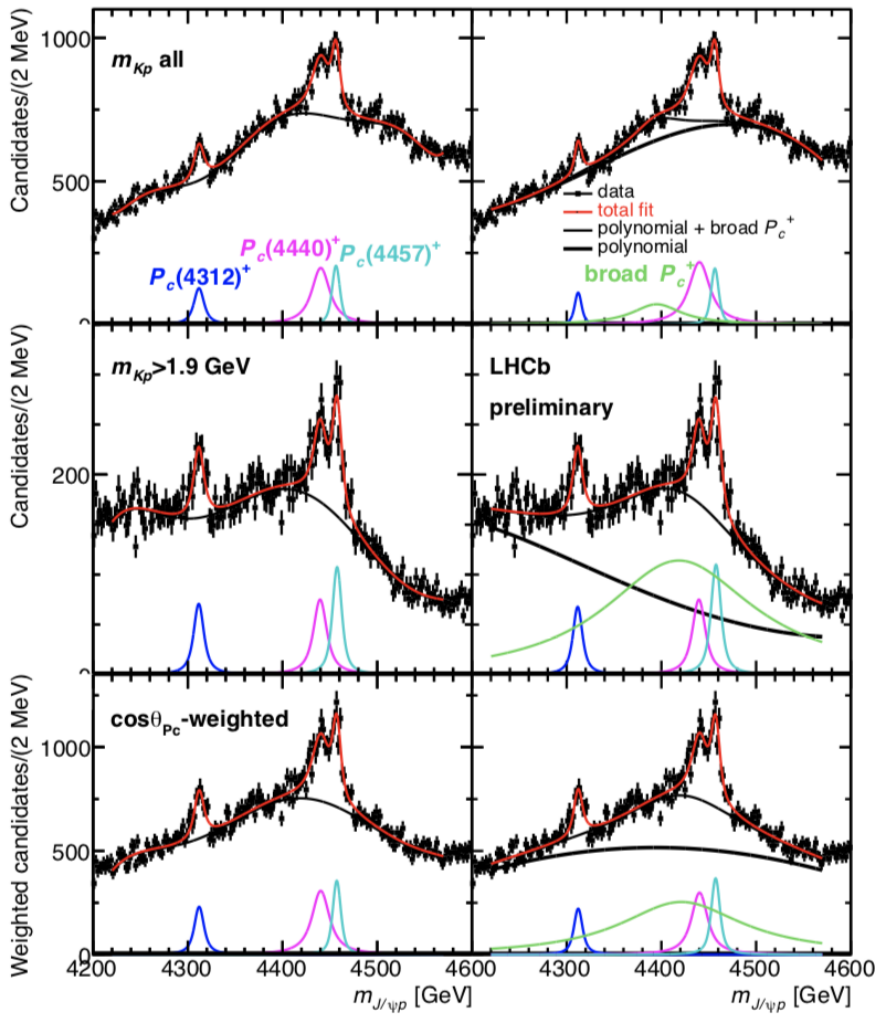

Results [LHCb-PAPER-2019-014 (in preparation)]

$$\mathcal{R} \equiv \frac{\mathcal{B}(\Lambda_b^0 \to P_c^+ K^-)\mathcal{B}(P_c^+ \to J/\psi K^-)}{\mathcal{B}(\Lambda_b^0 \to J/\psi p K^-)}$$

State	M [MeV]	Γ [MeV]	(95% CL)	$\mathcal{R}$ [%]
$P_c(4312)^+$	$4311.9 \pm 0.7^{+6.8}_{-0.6}$	$9.8 \pm 2.7^{+\ 3.7}_{-\ 4.5}$	(< 27)	$0.30 \pm 0.07^{+0.34}_{-0.09}$
$P_c(4440)^+$	$4440.3 \pm 1.3^{+4.1}_{-4.7}$	$20.6 \pm 4.9^{+\ 8.7}_{-10.1}$	(< 49)	$1.11 \pm 0.33^{+0.22}_{-0.10}$
$P_c(4457)^+$	$4457.3 \pm 0.6^{+4.1}_{-1.7}$	$6.4 \pm 2.0^{+\ 5.7}_{-\ 1.9}$	(< 20)	$0.53 \pm 0.16^{+0.15}_{-0.13}$

- $P_c(4312)^+$, $P_c(4440)^+$ not near triangle diagram thresholds, $P_c(4457)^+$ close to $\Lambda_c^+ \bar{D}^0$ threshold
- Data are described better by a BW wrt the triangle-diagram term
- Narrow widths and masses close to $\Sigma_c^+ \bar{D}^0$ and $\Sigma_c^+ \bar{D}^{*0}$ points toward bound states of a baryon and a meson

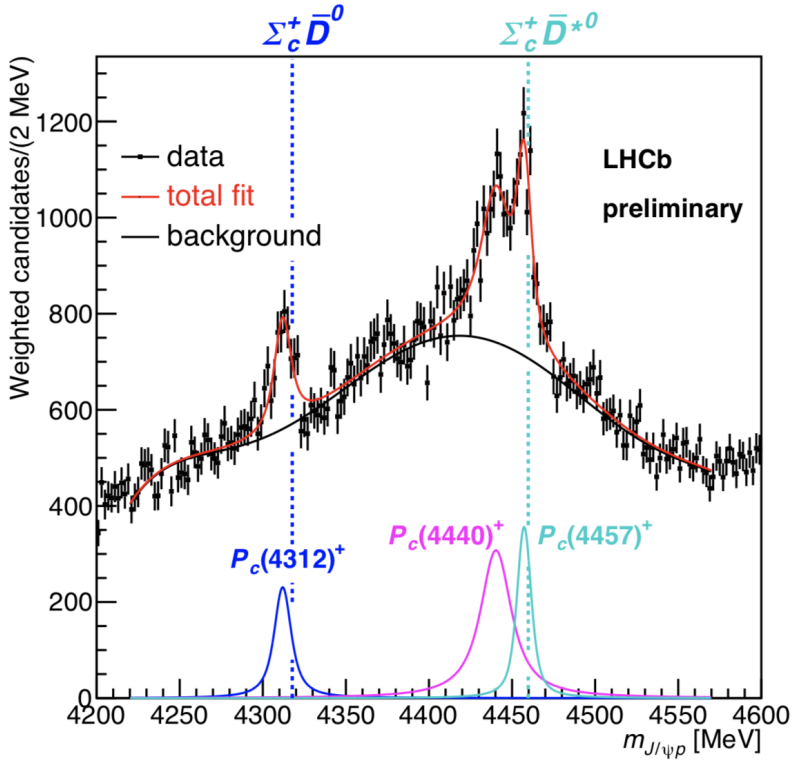

Standard spectroscopy

Near-threshold $D\bar{D}$ spectroscopy and observation of a new charmonium state
arXiv: 1903.12240, submitted to JHEP

New charmonium in $D\bar{D}$ [arXiv: 1903.12240]

- Run1 + Run2 data: $9\,\mathrm{fb}^{-1}$: first analysis using the complete dataset!
- Select promptly produced D^+D^- and $D^0\bar{D}^0$ candidates
- To reduce combinatorial background, exploit D meson decay time
- Select only D candidates with mass within $\pm 20\,\mathrm{MeV}$ (approximately $\pm 3\sigma$) of the known D-meson

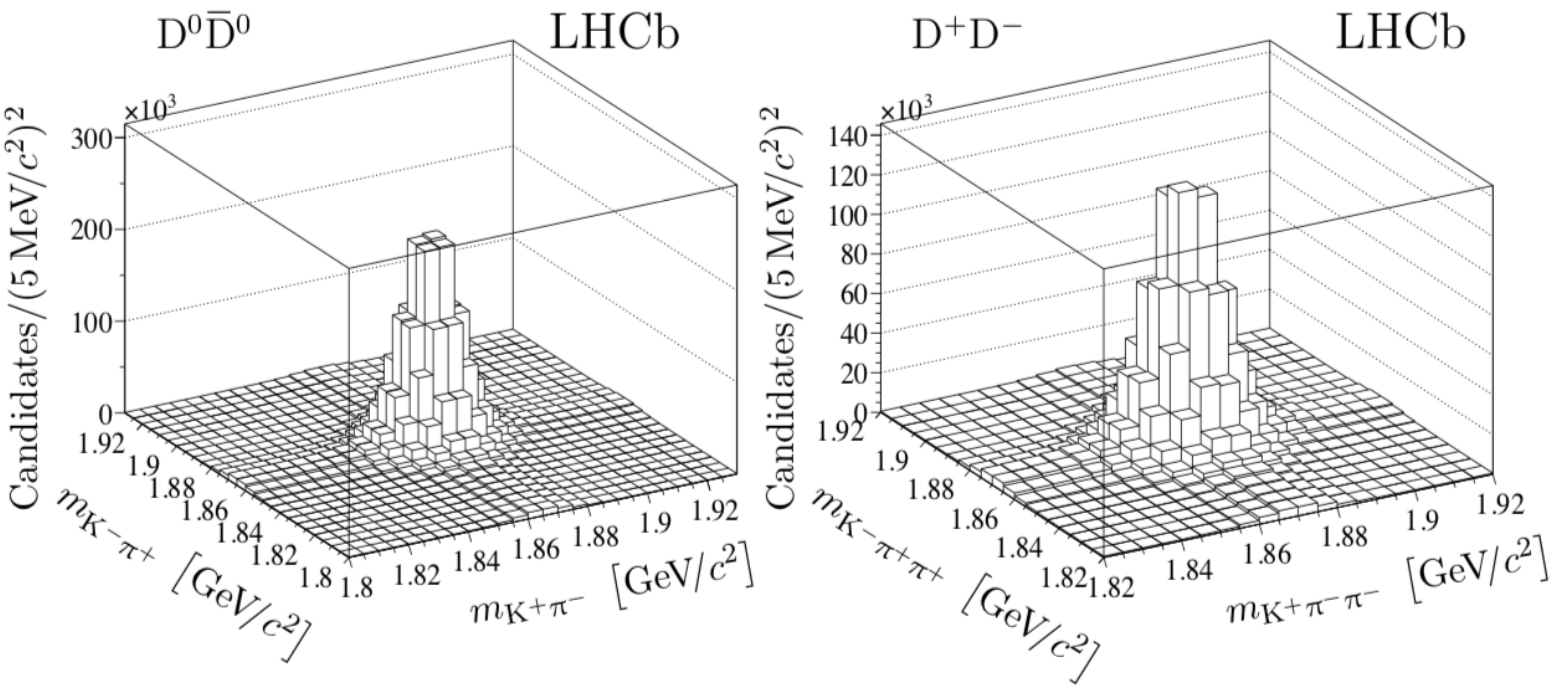

$D\bar{D}$ spectra [arXiv: 1903.12240]

- To improve $D\bar{D}$ resolution: D mass constrained to the known values
- To better model background fits performed in three different mass regions

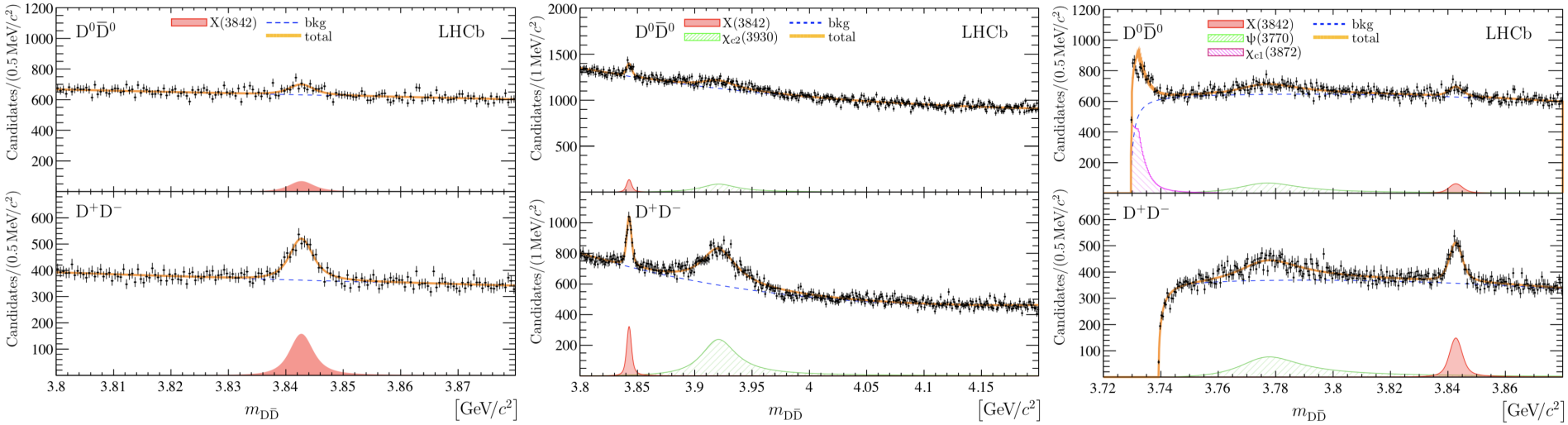

- New narrow charmonium state: X(3842), interpretation as $\psi_3(1^3D_3)$ with $J^{PC} = 3^{--}$

  $m = 3842.71 \pm 0.16 \pm 0.12\,\text{MeV} \quad \Gamma = 2.79 \pm 0.51 \pm 0.35\,\text{MeV}$

- First observation of hadroproduction of $\psi(3770)$ and of $\chi_{c2}(3930)$

  $m(\psi(3770)) = 3778.1 \pm 0.7 \pm 0.6\,\text{MeV}$

  $m(\chi_{c2}(3930)) = 3921.9 \pm 0.6 \pm 0.2\,\text{MeV}$

  $\Gamma(\chi_{c2}(3930)) = 36.6 \pm 1.9 \pm 0.9\,\text{MeV}$

$D\bar{D}$ results [arXiv: 1903.12240]

	$m_{\chi_{c2}(3930)}$ [MeV/c^2]	$\Gamma_{\chi_{c2}(3930)}$ [MeV]
Belle PRL 96 (2006) 082003	$3929 \pm 5 \pm 2$	$29 \pm 10 \pm 2$
BaBar PRD 81 (2010 092003	$3926.7 \pm 2.7 \pm 1.1$	$21.3 \pm 6.8 \pm 3.6$
This analysis	$3921.9 \pm 0.6 \pm 0.2$	$36.6 \pm 1.9 \pm 0.9$

	$m_{\psi(3770)}$ [MeV/c^2]
Shamov and Todyshev PLB 769 (2017) 187	3779.8 ± 0.6
PDG average	3778.1 ± 1.2
PDG fit	3773.13 ± 0.35
This analysis	$3778.1 \pm 0.7 \pm 0.6$

- The mass of the $\chi_{c2}(3930)$ is 2σ lower than the current world average
- The natural width of the $\chi_{c2}(3930)$ is 2σ higher than the current world average
- Mass value is midway between the mass for this state and for the X(3915) meson: two distinct charmonium states in this region or only one? [PRL 115 (2015) 0220001]
- Good agreement for the mass of the $\psi(3770)$

Mass and production measurement of Ξ_b^- baryons

PRD 99, 052006 (2019)

Mass and production of Ξ_b^- [PRD 99, 052006 (2019)]

- Thanks to the large $b\bar{b}$ production cross-section at LHC, b-hadrons new decay modes and new states have been observed
- In order to measure their branching fractions fragmentation fractions are needed
- $f_{\Xi_b^0}$, $f_{\Xi_b^-}$ and $f_{\Omega_b^-}$ are not known
- Exploit the decays $\Lambda_b^0 \to J/\psi\Lambda$ and $\Xi_b^- \to J/\psi\Xi^-$
- Using SU(3) flavor symmetry

$$\frac{\Gamma(\Xi_b^- \to J/\psi\Xi^-)}{\Gamma(\Lambda_b^0 \to J/\psi\Lambda)} = \frac{3}{2}$$

$$\frac{f_{\Xi_b^-}}{f_{\Lambda_b^0}} \frac{\mathcal{B}(\Xi_b^- \to J/\psi\Xi^-)}{\mathcal{B}(\Lambda_b^0 \to J/\psi\Lambda)} = \frac{f_{\Xi_b^-}}{f_{\Lambda_b^0}} \frac{\Gamma(\Xi_b^- \to J/\psi\Xi^-)}{\Gamma(\Lambda_b^0 \to J/\psi\Lambda)} \frac{\tau_{\Xi_b^-}}{\tau_{\Lambda_b^0}} = \frac{N(\Xi_b^- \to J/\psi\Xi^-)}{N(\Lambda_b^0 \to J/\psi\Lambda)} \frac{\epsilon_{\Lambda_b^0}}{\epsilon_{\Xi_b^-}}$$

- Using 1, 2 and $1.6\,\mathrm{fb}^{-1}$ at $\sqrt{s} = 7$, 8 and $13\,\mathrm{TeV}$
- First measurement of the production rate of Ξ_b^- baryons in pp collisions

Mass and production of Ξ_b^- [PRD 99, 052006 (2019)]

$\Lambda_b^0 \to J/\psi\Lambda$

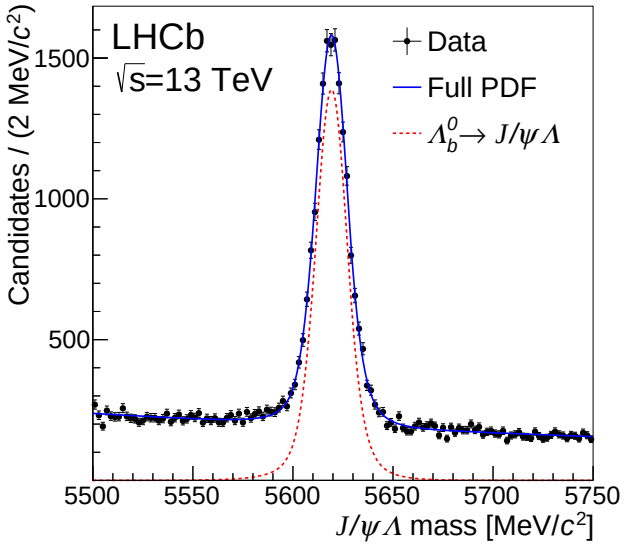

$\Xi_b^- \to J/\psi\Xi^-$
inside the vertex locator detector

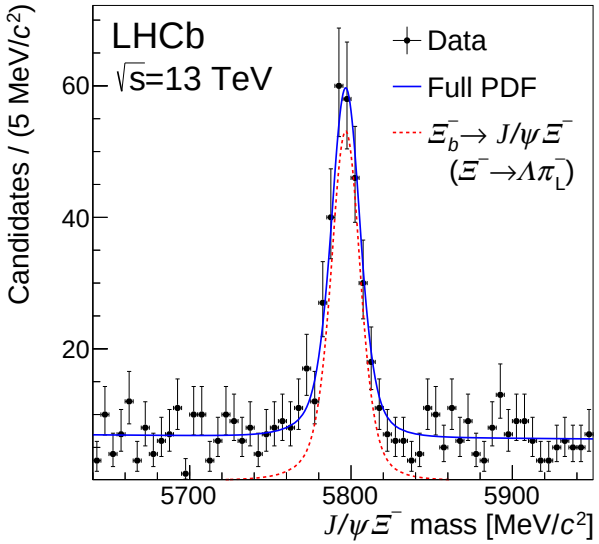

$\Xi_b^- \to J/\psi\Xi^-$
outside the vertex locator detector

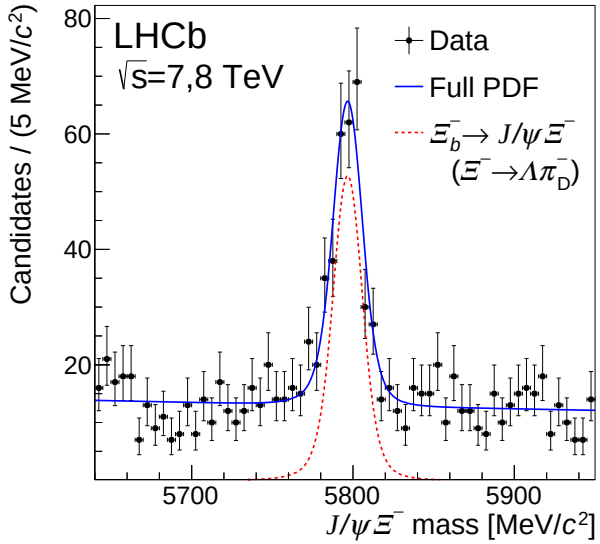

$$f_{\Xi_b^-}/f_{\Lambda_b^0} = (6.7 \pm 0.5(\text{stat}) \pm 0.5(\text{syst}) \pm 2.0(\text{SU(3)breaking})) \times 10^{-2} \text{at} \sqrt{s} = 7,8\,\text{TeV}$$

$$f_{\Xi_b^-}/f_{\Lambda_b^0} = (8.2 \pm 0.7(\text{stat}) \pm 0.6(\text{syst}) \pm 2.5(\text{SU(3)breaking})) \times 10^{-2} \text{at} \sqrt{s} = 13\,\text{TeV}$$

- No significant dependence on the center-of-mass energy (7 to 13 TeV range)

$$m(\Xi_b^-) = 5796.70 \pm 0.39 \pm 0.15 \pm 0.17\,\text{MeV}$$

- Most precise measurement of the mass
- Production asymmetry consistent with zero at the level of few percent

B_c physics

- B_c mesons formed by two different heavy quarks, unique in the SM
- B_c^+ discovered by CDF at Tevatron [PRL 81 (1998) 2432]
- Expected rich spectrum predicted by QCD potential models and Lattice QCD
- Spectroscopy observations are scarce due to low cross-sections and large backgrounds
- States below BD threshold can only undergo radiative or pionic transitions to the ground state B_c^+ which decays weakly

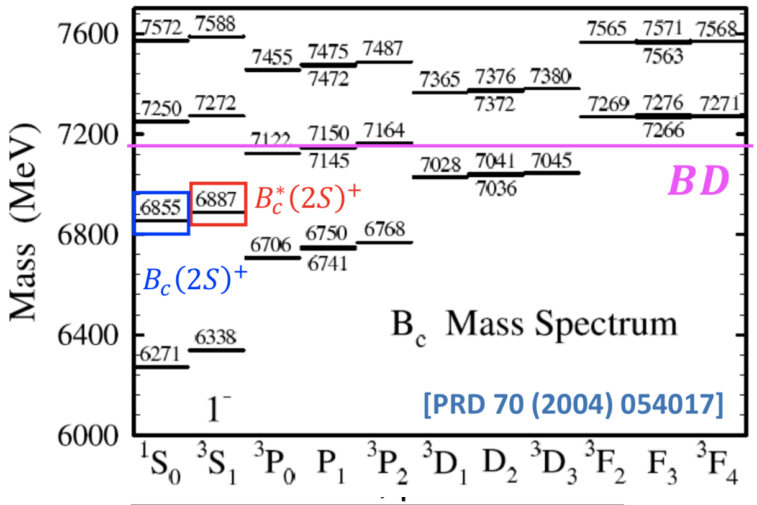

State	Decay	GKLRY *	Godfrey †
1^3S_1	$1^1S_0+\gamma$	100	100
1^3P_2	$1^3S_1+\gamma$	100	100
$1P_1'$	$1^3S_1+\gamma$	6	12.1
	$1^1S_0+\gamma$	94	87.9
$1P_1$	$1^3S_1+\gamma$	87	82.2
	$1^1S_0+\gamma$	13	17.8
1^3P_0	$1^3S_1+\gamma$	100	100
2^1S_0	$1^1S_0+\pi\pi$	74	88.1
	$1P_1'+\gamma$		9.4
	$1P_1+\gamma$		2.0
	$1^3S_1+\gamma$		0.5
2^3S_1	$1^3S_1+\pi\pi$	58	79.6
	$1^3P_2+\gamma$		8.0
	$1P_1'+\gamma$		1.0
	$1P_1+\gamma$		6.6
	$1^3P_0+\gamma$		4.0
	$2^1S_0+\gamma$		0.01
	$1^1S_0+\gamma$		0.8

*. Gouz, Phys.Atom.Nucl.67(2004) 1559
† Godfrey, PRD 70 (2004) 054017

$B_c^*(2S)$ and $B_c(2S)$ states

- Main decay modes:
  - $B_c(2S) \to B_c\pi^+\pi^-$
  - $B_c^*(2S) \to B_c^*(\to B_c\gamma)\pi^+\pi^-$ with low energy photon (which is not reconstructed)
- Both states can be observed reconstructing $B_c\pi^+\pi^-$ with the $B_c^{*+}(2S)$ at the mass $M(B_c^+(2S))_{\rm rec} = M(B_c^+(2S)) - M(B_c^{*+}) - M(B_c^+)$
- From predictions $M(B_c^{*+}) - M(B_c^+) > M(B_c^{*+}(2S)) - M(B_c^+(2S))$
- Then $M(B_c^+(2S)) > M(B_c^{*+}(2S))_{\rm rec}$

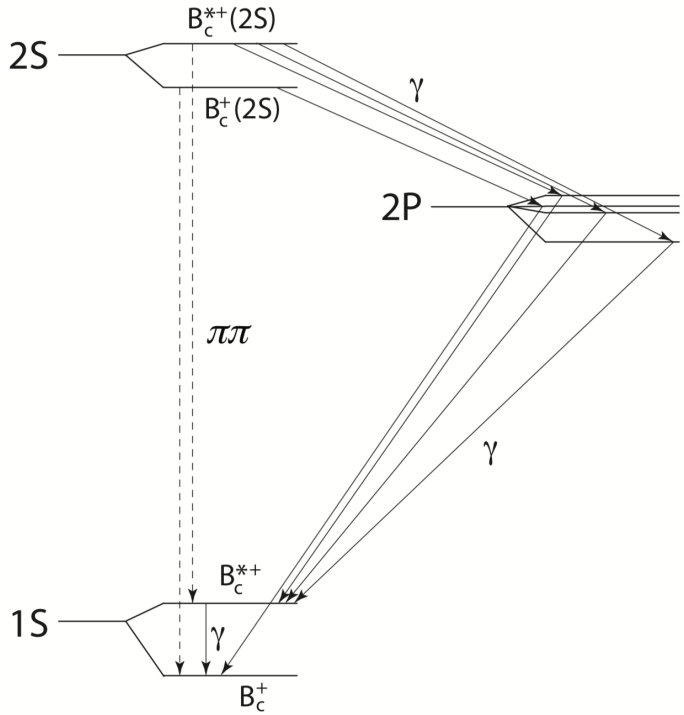

Excited B_c^+ states at ATLAS PRL 113 (2014) 12004

- Observation of an excited B_c meson state with a significance of 5.2σ
- Data sample: full Run1 data
- Reconstructed in $B_c^+\pi^+\pi^-$ with $B_c \to J/\psi\pi^+$
- Measured mass $M = 6842 \pm 4 \pm 5\,\mathrm{MeV}$ consistent with expectations of the $B_c(2S)$
- Both the 1S and 2S states have pseudoscalar (0^-) and vector (1^-) spin states with mass predictions that differ by about 20-50 MeV
- No discrimination between $B_c^+(2S)$ and $B_c^{*+}(2S)$ (soft photon)
- Probably a superposition of the $B_c^+(2S)$ and $B_c^{*+}(2S)$: two peaks unresolved

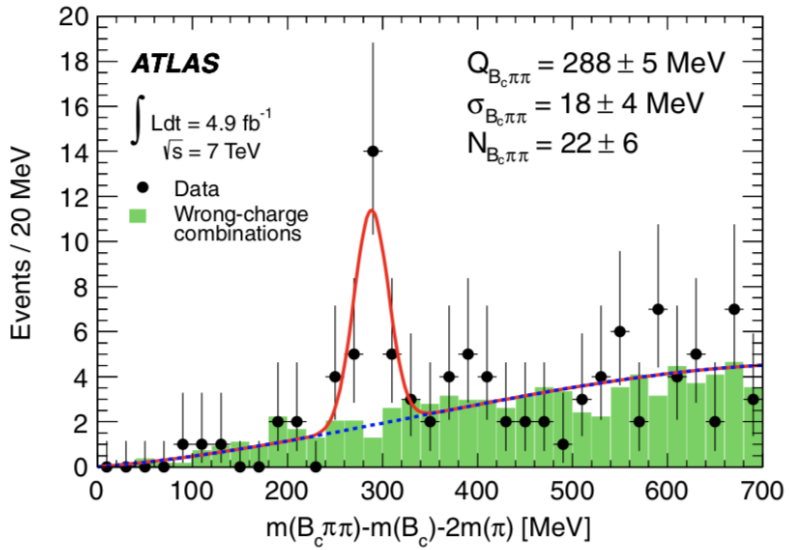

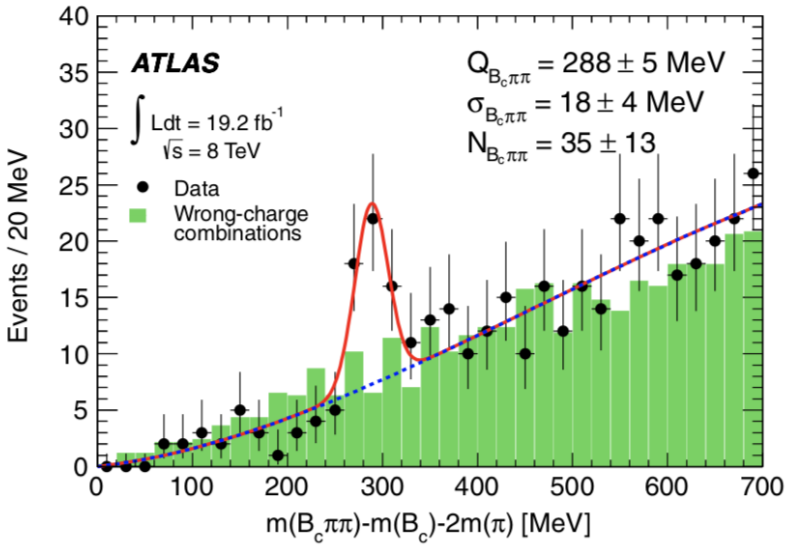

Excited B_c^+ states at CMS [arXiv:1902.00571, submitted to PRL]

- Full $140\,\mathrm{fb}^{-1}$ Run2 data
- Using $B_c^+ \to J/\psi(\mu\mu)\pi$ decay
- High-p_T B_c^+ candidates ($p_\mathrm{T} > 15\,\mathrm{GeV}$)
- Well-separated $B_c(2S)$ and $B_c^*(2S)$ peaks, both observed and resolved with significance $> 5\sigma$

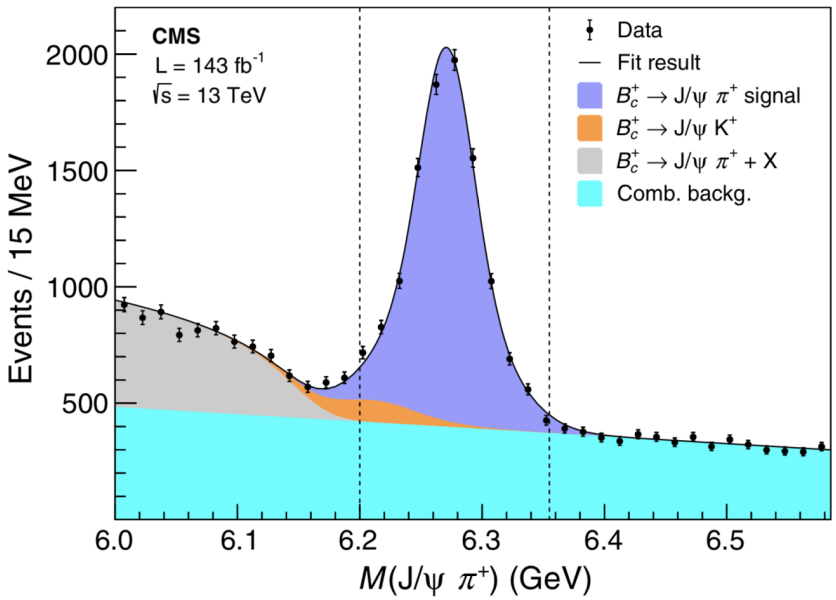

$N(B_c^+) = 7629 \pm 226$

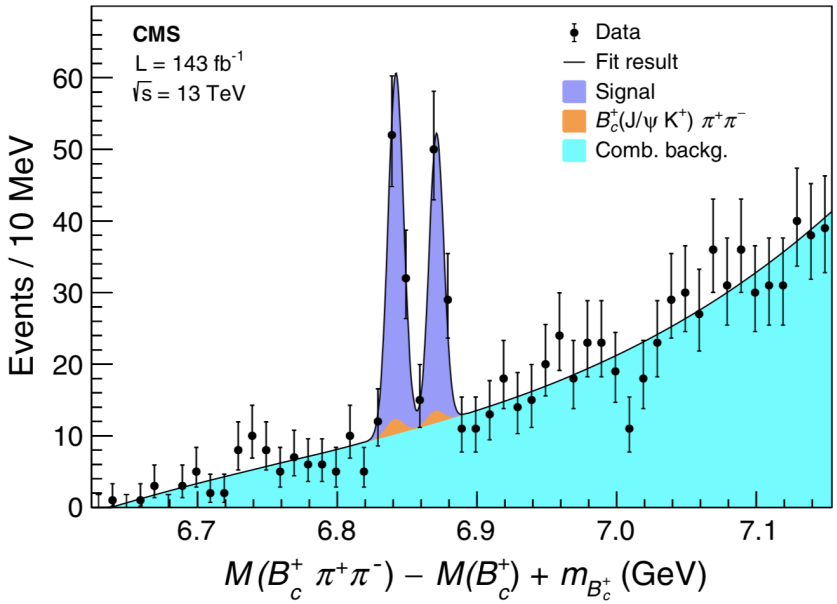

$N(B_c^*(2S)^+) = 67 \pm 10$
$N(B_c(2S)^+) = 51 \pm 10$

$$M(B_c(2S)^+) = 6871.0 \pm 1.2(stat) \pm 0.8(syst) \pm 0.8(B_c^+)\,\mathrm{MeV}$$
$$M(B_c(2S)^+) - M(B_c^*(2S)^+)_\mathrm{rec} = 29.1 \pm 1.5(stat) \pm 0.7(syst)\,\mathrm{MeV}$$

$B_c^{(*)}(2S)^+$ at LHCb [arXiv:1904.00081, Submitted to PRL]

- Data sample with $8.5\,\text{fb}^{-1}$ Run1 +Run2 data
- Requirements: $p_{\text{T}}(B_c^+) > 10\,\text{GeV}$, $p_{\text{T}}(\pi^+) > 300\,\text{MeV}$
- $B_c^*(2S)^+$ observed with significance $> 5\sigma$
- Hint for $B_c(2S)^+$ with global (local) significance of $2.2(3.2)\sigma$

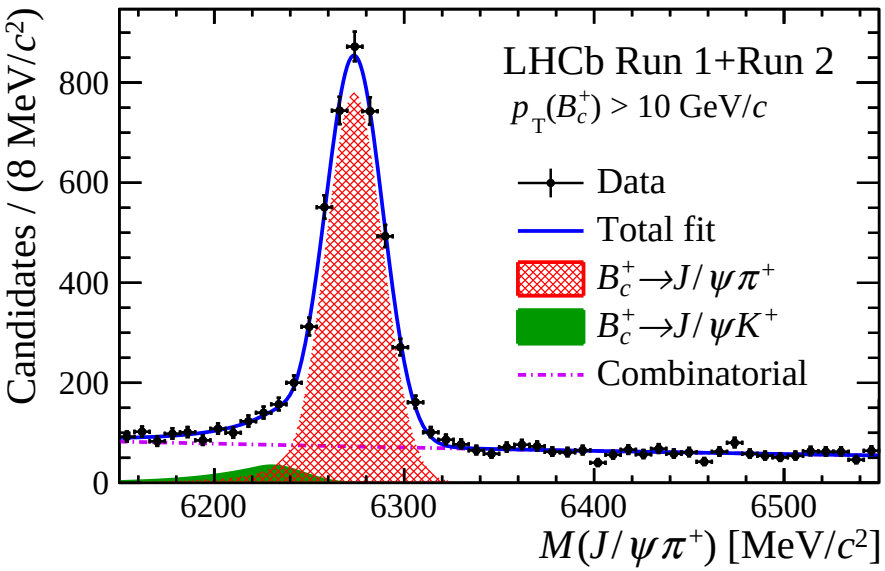

$N(B_c) = 3785 \pm 73$

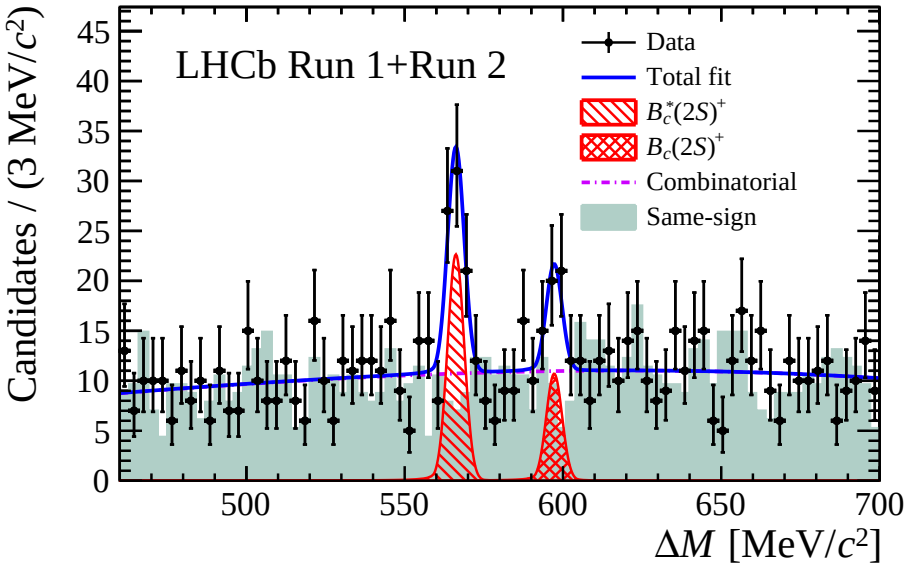

$N(B_c^*(2S)^+) = 51 \pm 10$
$N(B_c(2S)^+) = 24 \pm 9$

$$M(B_c^*(2S)^+)_{\text{rec}} = 6841.2 \pm 0.6(stat) \pm 0.1(syst) \pm 0.8(B_c^+)\,\text{MeV}$$
$$M(B_c(2S)^+) = 6872.1 \pm 1.3(stat) \pm 0.1(syst) \pm 0.8(B_c^+)\,\text{MeV}$$
$$M(B_c(2S)^+) - M(B_c^*(2S)^+)_{\text{rec}} = 31.0 \pm 1.4(stat)\,\text{MeV}$$

Conclusions

- Wide range of interesting spectroscopy results: only a small selection of recent results
- Continuing to exploit LHC experiment potential adding Run2 data
  - Updates of present analyses with higher stats, precision measurements
  - More amplitude analysis
  - Exotic states searches in other decay channels
- Long Shutdown 2 started, the detectors are going to be upgraded: collect a larger data sample with high efficiency starting in 2021!

Spare slides

Weight function

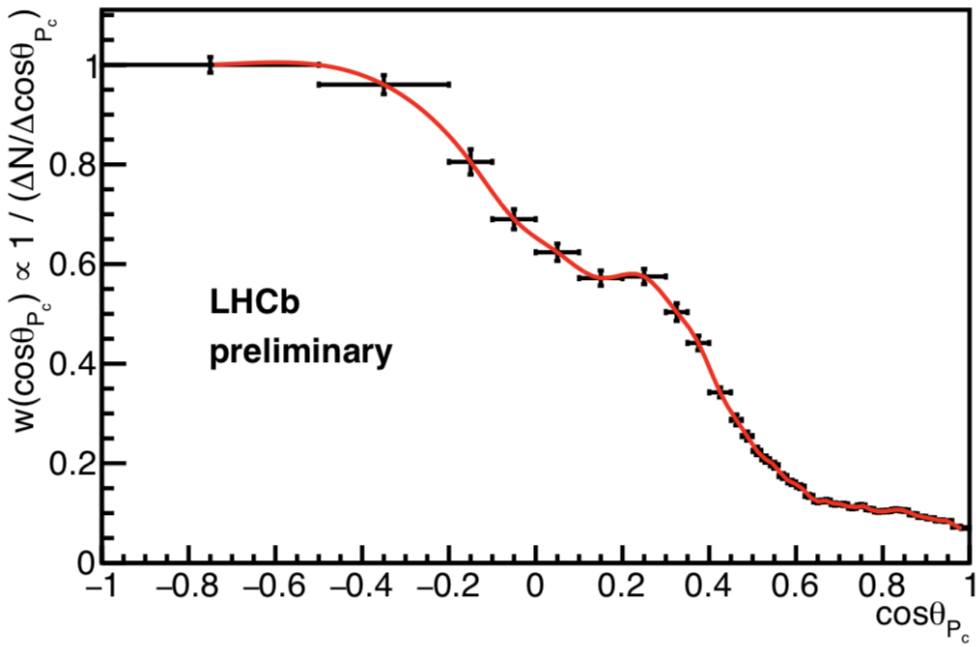

Weight function $\cos\theta_P$ (where θ_P is the angle between the K^- and the J/ψ in the P_c^+ rest frame (helicity angle)) determined as the inverse of the density of Λ_b^0 candidates in the narrow P_C^+ peak region. The red line is the spline used to interpolate between bin centers. The Λ^* backgrounds mostly populate the $\cos\theta_{P_C} > 0$ region. The weights are taken to be the inverse of the expected background which is approximately given by the density of candidates observed in data since the signal contributions are small.

Triangle diagram

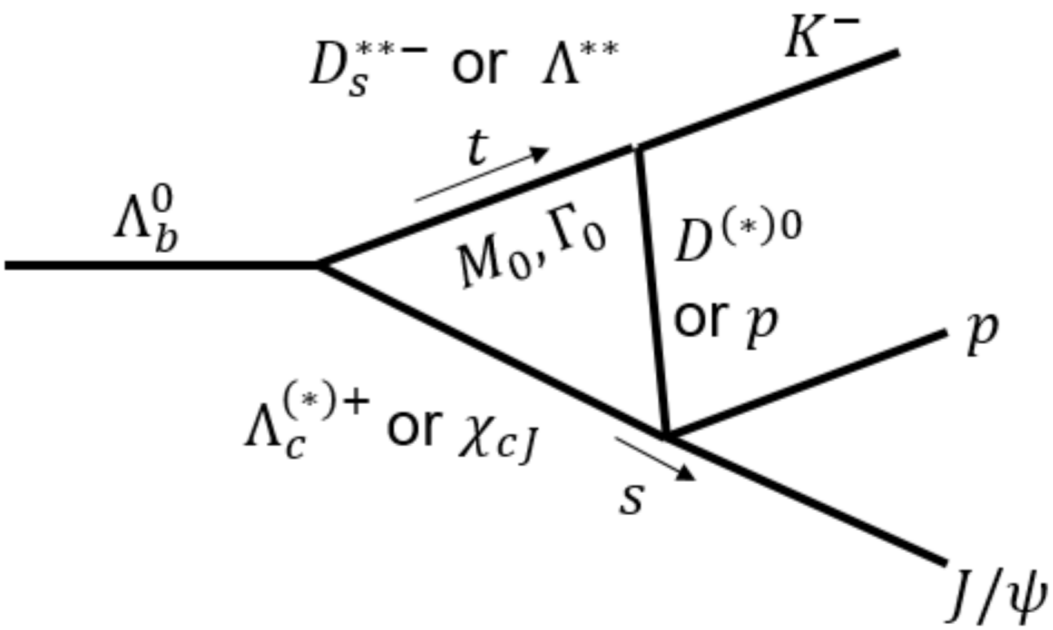

The Λ_b baryon decays into two nearly on-mass-shell hadrons, one of which is an excited strange meson or baryon that emits a kaon and a non-strange decay product that rescatters with the other Λ_b^0 child into the $J/\psi p$ system. These processes are know to peak when all three hadrons in the triangle are nearly on their mass shell.

Triangle diagram

- $P_c(4457)^+$ peaks near the $\Lambda_c^+(2595)\bar{D}^0$ threshold with the emission of the $D_{s1}(2860)^-$ meson
- $P_c(4312)^+$ is not far from the $\Lambda_c^+\bar{D}^{*0}$ threshold (with the emission of the excited 1^- D_s^{**} meson but no narrow peak
- $P_c(4440)^+$ well above the $\chi_{c0}p$ threshold with the emission of Λ^* but no narrow peak

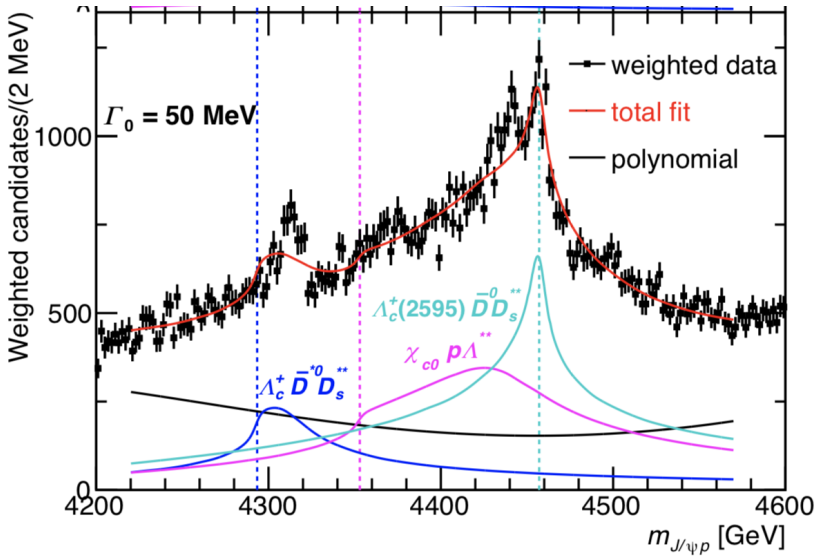

The LHCb detector

Designed to study CP-violating processes and rare b- and c-hadrons decays

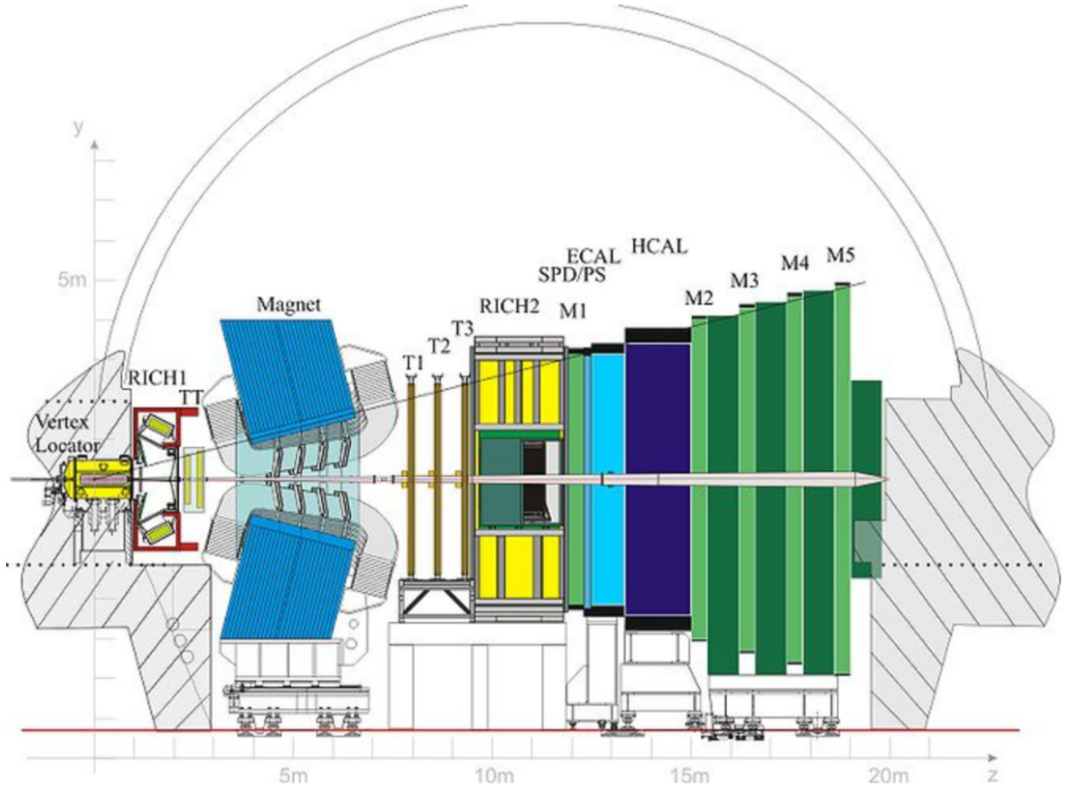

Impact parameter:	$\sigma_{IP} = 20\ \mu m$
Proper time:	$\sigma_\tau = 45$ fs for $B_s^0 \to J/\psi\phi$ or $D_s^+\pi^-$
Momentum:	$\Delta p/p = 0.4 \sim 0.6\%$ (5 – 100 GeV/c)
Mass :	$\sigma_m = 8\ \mathrm{MeV}/c^2$ for $B \to J/\psi X$ (constrainted $m_{J/\psi}$)
RICH $K-\pi$ separation:	$\epsilon(K \to K) \sim 95\%$ mis-ID $\epsilon(\pi \to K) \sim 5\%$
Muon ID:	$\epsilon(\mu \to \mu) \sim 97\%$ mis-ID $\epsilon(\pi \to \mu) \sim 1-3\%$
ECAL:	$\Delta E/E = 1 \oplus 10\%/\sqrt{E(\mathrm{GeV})}$

Interpretations of exotic hadrons

- Different models have been proposed about the quark composition and binding mechanisms of these exotic hadrons

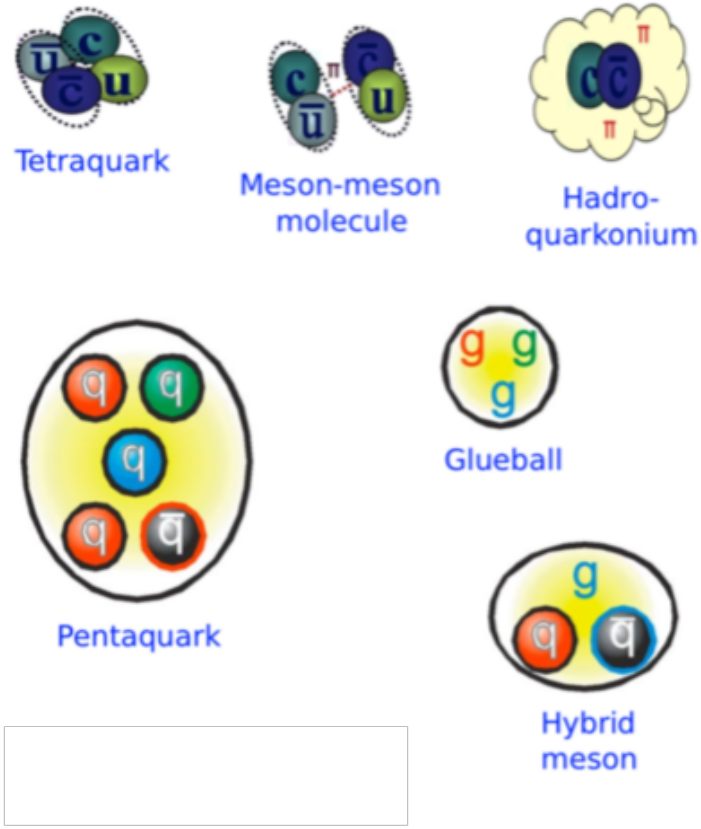

Predictions of a $\eta_c\pi^-$ exotic state

- $Z_c(3900)^-$ as hadrocharmonium state (where the compact heavy quark-antiquark pair interacts with the surrounding light quark mesonic excitation by a QCD analogue of the van der Waals force): predicts an as-yet-unobserved charged charmonium-like state with a mass of approximately $3800\,\mathrm{MeV}$ whose dominant decay mode is to the $\eta_c\pi^-$ system
- $Z_c(3900)^-$ as quarkonium hybrids where the excitation of the gluon field (the valence gluon) is replaced by an isospin-1 excitation of the gluon and light-quark fields
  - prediction of different multiplets of charmonium tetraquarks, comprising states with quantum numbers allowing the decay into the $\eta_c\pi^-$ system.
  - The $\eta_c\pi^-$ system carries isospin $I = 1$, G-parity $G = 1$, spin $J = L$ and parity $P = (-1)^L$, where L is the orbital angular momentum between the η_c and the π^- mesons. Lattice QCD calculations predict the mass and quantum numbers of these states, comprising a $I^G(J^P) = 1(0^+)$ state of mass $4025 \pm 49\,\mathrm{MeV}$, a $I^G(J^P) = 1^-(1^-)$ state of mass $3770 \pm 42\,\mathrm{MeV}$, and a $I^G(J^P) = 1^-(2^+)$ state of mass $4045 \pm 44\,\mathrm{MeV}$. The $Z_c(4430)$ resonance, discovered by the Belle collaboration and confirmed by LHCb, could also fit into this scenario.
- Diquark model: a $J^P = 0^+$ exotic candidate below the open-charm threshold decaying to $\eta_c\pi^-$

Parametrisation of the backgrounds

- sPlot technique from the joint 2D $m(p\bar{p}K^+\pi^-), m(p\bar{p})$ fit is used to extract combinatorial and NR background histograms
- Smoothing procedure using a 2D cubic spline interpolation
- Parametrised using the Square Dalitz plot (SDP) using the variables m' and θ' defined in the range 0 to 1 and given by

$$m' \equiv \frac{1}{\pi}\arccos\left(2\frac{m(K^+\pi^-)-m^{\min}_{K^+\pi^-}}{m^{\max}_{K^+\pi^-}-m^{\min}_{K^+\pi^-}}-1\right) \qquad \theta' \equiv \frac{1}{\pi}\theta(K^+\pi^-)$$

where $m^{\max}_{K^+\pi^-} = m_{B^0} - m_{\eta_c}$, $m^{\min}_{K^+\pi^-} = m_{K^+} + m_{\pi^-}$ and $\theta(K^+\pi^-)$ is the helicity angle of the $K^+\pi^-$ system (the angle between the K^+ and the η_c mesons in the $K^+\pi^-$ rest frame

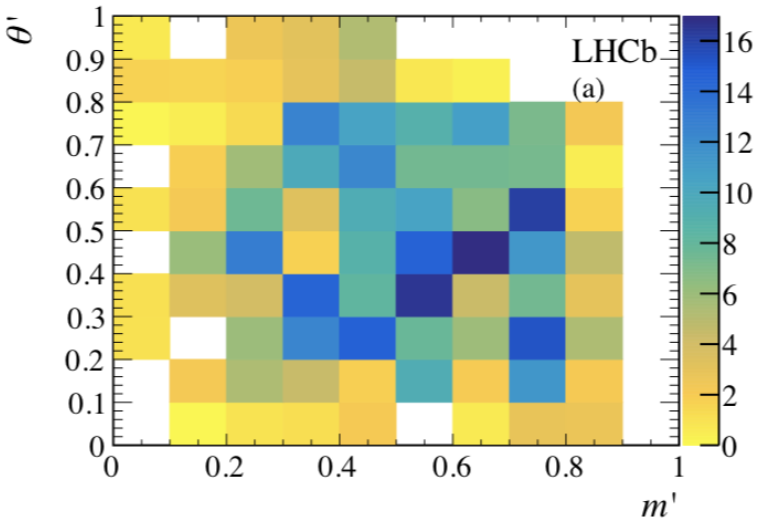

Combinatorial bkg

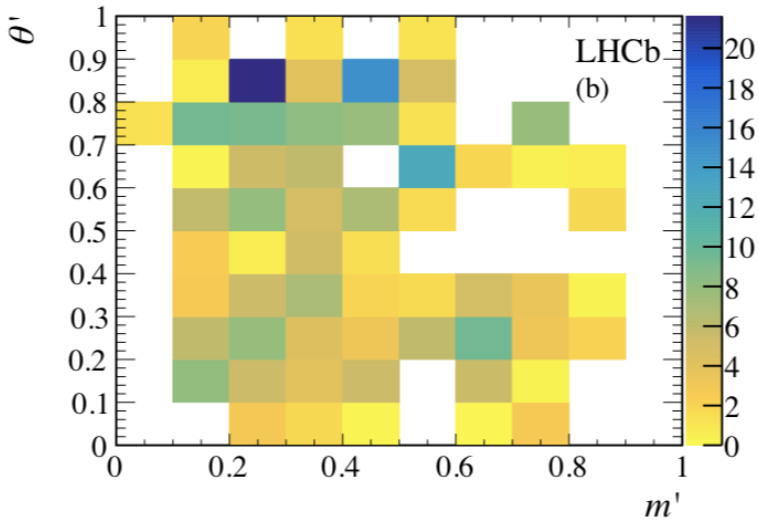

NR bkg

Efficiency

- Efficiency variation across the SDP caused by the detector acceptance and by the trigger and offline selection requirements
- Evaluated with simulated samples generated uniformly across the SDP.
- Corrections are applied for known differences between data and simulation
- Efficiency studied separately for the Run1 and Run2 subsamples
- Smoothing procedure using a 2D cubic spline interpolation

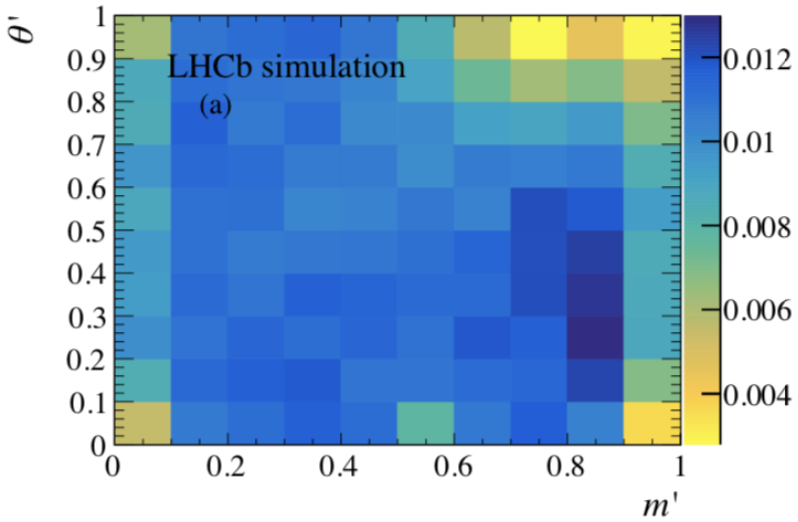

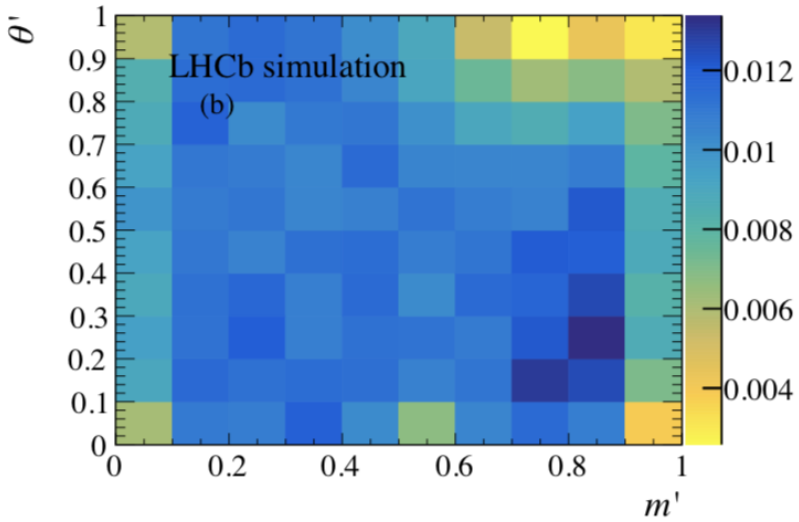

Cross-checks

- No significant improvement adding further high-mass K^{*0} states ($K_3^*(1780)^0$, $K_4^*(2045)^0$, the high mass $K_5^*(2380)^0$ which falls outside the phase space limits, the $K_2^*(1980)^0$ which has not been seen in the $K^+\pi^-$ final state thus far and the unestablished P-, D- and F-wave $K^+\pi^-$ states predicted by the GodfreyIsgur model)
- No significant additional amplitude decaying to $\eta_c\pi^-$
- No significant additional exotic amplitude decaying to $\eta_c K^+$
- Noegligible effect due to the variation of the η_c phase due to the sizeable natural width introducing interference effects with the NR $p\bar{p}$ contribution [data sample is divided in two, containing candidates with masses below and above the η_c meson peak]

Quasi-two-body branching fractions

Amplitude	Fit fraction (%)
$B^0 \to \eta_c K^*(892)^0$	$51.4 \pm 1.9\ ^{+1.7}_{-4.8}$
$B^0 \to \eta_c K^*(1410)^0$	$2.1 \pm 1.1\ ^{+1.1}_{-1.1}$
$B^0 \to \eta_c K^+\pi^-$ (NR)	$10.3 \pm 1.4\ ^{+1.0}_{-1.2}$
$B^0 \to \eta_c K_0^*(1430)^0$	$25.3 \pm 3.5\ ^{+3.5}_{-2.8}$
$B^0 \to \eta_c K_2^*(1430)^0$	$4.1 \pm 1.5\ ^{+1.0}_{-1.6}$
$B^0 \to \eta_c K^*(1680)^0$	$2.2 \pm 2.0\ ^{+1.5}_{-1.7}$
$B^0 \to \eta_c K_0^*(1950)^0$	$3.8 \pm 1.8\ ^{+1.4}_{-2.5}$
$B^0 \to Z_c(4100)^- K^+$	$3.3 \pm 1.1\ ^{+1.2}_{-1.1}$

Decay mode	Branching fraction (10^{-5})
$B^0 \to \eta_c K^*(892)^0$	$29.5 \pm 1.6 \pm 0.6\ ^{+1.0}_{-2.8} \pm 3.4$
$B^0 \to \eta_c K^*(1410)^0$	$1.20 \pm 0.63 \pm 0.02 \pm 0.63 \pm 0.14$
$B^0 \to \eta_c K^+\pi^-$ (NR)	$5.90 \pm 0.84 \pm 0.11\ ^{+0.57}_{-0.69} \pm 0.68$
$B^0 \to \eta_c K_0^*(1430)^0$	$14.50 \pm 2.10 \pm 0.28\ ^{+2.01}_{-1.60} \pm 1.67$
$B^0 \to \eta_c K_2^*(1430)^0$	$2.35 \pm 0.87 \pm 0.05\ ^{+0.57}_{-0.92} \pm 0.27$
$B^0 \to \eta_c K^*(1680)^0$	$1.26 \pm 1.15 \pm 0.02\ ^{+0.86}_{-0.97} \pm 0.15$
$B^0 \to \eta_c K_0^*(1950)^0$	$2.18 \pm 1.04 \pm 0.04\ ^{+0.80}_{-1.43} \pm 0.25$
$B^0 \to Z_c(4100)^- K^+$	$1.89 \pm 0.64 \pm 0.04\ ^{+0.69}_{-0.63} \pm 0.22$

Width of the $\eta_c(1S)$

- Necessary to take into account the sizeable natural width of the $\eta_c(1S)$ meson ($\Gamma \sim 32\,\mathrm{MeV}$):
  - Kinematic quantities such as $m^2(K^+\pi^-)$, $m^2(\eta_c\pi^-)$ and the helicity ancles are calculated using the invariant mass $m(p\bar{p})$ instead of the known value of the η_c mass
  - When computing the DP normalisation the width of the η_c meson is set to zero: the effect of this simplification is determined when assessing the systematic uncertainties
  - Amplitude fits are repeated computing the DP normalisations by using the $m_{\eta_c} + \Gamma_{\eta_c}$ and $m_{\eta_c} - \Gamma_{\eta_c}$

LASS model

- The amplitude parametrisations using RBW functions lead to unitarity violation within the isobar model if there are overlapping resonances or if there is a significant interference with a NR component, both in the same partial wave
- For the $K^+\pi$ S-wave at low $K^+\pi$ mass, where the $K_0(1430)^0$ resonance interferes strongly with a slowly varying NR S-wave component: LASS lineshape

$$T(m) = \frac{m}{|\vec{q}|\cot\delta_B - i|\vec{q}|} + e^{2i\delta_B}\frac{m_0\Gamma_0\frac{m_0}{q_0}}{m_0^2 - m^2 - im_0\Gamma_0\frac{|\vec{q}|}{m}\frac{m_0}{q_0}}$$

$$\cot\delta_B = \frac{1}{a|\vec{q}|} + \frac{1}{2}r|\vec{q}|$$

and where m_0 and Γ_0 are the pole mass and width of the $K_0(1430)^0$ state, and a and r are the scattering length and the effective range, respectively.

- The LASS model replaced with $K_0^*(1430)^0$ and $K_0^*(800)^0$ resonances parametrised with RBW functions, and a NR S-wave $K^+\pi^-$ component parametrised with a uniform amplitude within the DP.

Systematic uncertainties

- Experimental uncertainties
  - Fixed signal and background yields
  - background parametrisation
  - phase-space border veto applied on the parametrisation of the efficiencies
  - amplitude fit bias
- Model uncertainties
  - treatment of the $\eta_c(1S)$ natural width
  - $K^+\pi^-$ s-wave parametrisation
  - fixed parameters of the resonances
  - addition or removal of marginal components

- The systematic variations producing the largest deviations on the $Z_c(4100)$ parameters (mass, width and fit fraction) are used to evaluate the systematic effects on the significances
- $Z_c(4100)$ significance when including systematic uncertainties and correlations between them: 3.2σ

Source	$\Delta(-2\ln\mathcal{L})$	Significance
Nominal fit	41.4	4.8σ
Fixed yields	45.8	5.2σ
Phase-space border veto	44.6	5.1σ
η_c width	36.6	4.3σ
$K^+\pi^-$ S-wave	31.8	3.9σ
Background	27.4	3.4σ

Discrimination between $J^P = 0^+$ and $J^P = 1^-$

Source	$\Delta(-2\ln\mathcal{L})$	Significance
Default	18.6	4.3σ
Fixed yields	23.8	4.9σ
Phase-space border veto	24.4	4.9σ
η_c width	4.2	2.0σ
Background	3.4	1.8σ
$K^+\pi^-$ S-wave	1.4	1.2σ